

LOW FREQUENCY RAMAN INVESTIGATION OF  
WATER AND AQUEOUS SOLUTIONS

CENTRE FOR NEWFOUNDLAND STUDIES

**TOTAL OF 10 PAGES ONLY  
MAY BE XEROXED**

(Without Author's Permission)

BERNARD CHARLES RICE









**LOW FREQUENCY RAMAN INVESTIGATION OF WATER AND  
AQUEOUS SOLUTIONS**

© Bernard Charles Rice, B.Sc.

A Thesis submitted in partial fulfillment  
of the requirements for the degree of  
Master of Science

Department of Chemistry  
Memorial University of Newfoundland  
St. John's, Newfoundland, Canada

March 1984

## ABSTRACT

The Raman spectra of water and aqueous salt solutions are presented in the form of a vibrational density of states,  $R(\omega)$ . This  $R(\omega)$  format reveals with greater definition the low frequency Raman bands due to polarizability changes in the weak bonds of intermolecular complexes. For pure water at 25°C, broad bands were observed at  $66\text{ cm}^{-1}$  and  $192\text{ cm}^{-1}$  due to hydrogen bond bending and stretching modes. High signal to noise ratios achieved by multiple scans permitted the construction of difference spectra which greatly assisted the measurement of peak frequencies and depolarization data. The  $192\text{ cm}^{-1}$  band in the spectrum of water was found to be slightly polarized while the remainder of spectrum exhibited largely depolarized features. The hydrogen bond stretching mode of water shifted  $6\text{ cm}^{-1}$  in  $\text{D}_2\text{O}$  and  $17\text{ cm}^{-1}$  in  $\text{H}_2^{18}\text{O}$ . This mode is interpreted as arising from oxygens moving about the hydrogen involved in the hydrogen bond but with the proton remaining closer to one of the oxygens. The effects of salts on the water spectrum have also been investigated. Most salts increase the relative intensity of the water spectrum although typical structure breakers cause a decrease in the relative intensity. New bands have also been observed when salts are added to water. Reorientation of the  $\text{CO}_3^{2-}$  ion give rise to a depolarized scattering at  $92\text{ cm}^{-1}$  in aqueous solutions. Polarized bands due to cation and anion hydrates have also been observed. The symmetric stretch of the  $\text{Mg}(\text{H}_2\text{O})_6^{2+}$  ion is observed at  $359\text{ cm}^{-1}$  in  $\text{MgCl}_2$  while a polarized band for  $\text{LiCl}_{(\text{aq})}$  occurs at  $384\text{ cm}^{-1}$ . Polarized bands at  $263\text{ cm}^{-1}$  for saturated  $\text{KF}_{(\text{aq})}$ ,  $298\text{ cm}^{-1}$  for  $10\text{M NaOH}_{(\text{aq})}$ ,  $293\text{ cm}^{-1}$  for  $11.5\text{M KOH}_{(\text{aq})}$ ,  $286\text{ cm}^{-1}$  for  $5.9\text{M RbOH}_{(\text{aq})}$  and in  $\text{CsOH}_{(\text{aq})}$  are assigned to stretching of the  $\text{O-H}\cdots\text{X}^-$  band.

**ACKNOWLEDGEMENTS**

The author wishes to thank Professor Murray H. Brooker for his continual guidance and supervision during the development of his work.

The author would also like to thank his wife Dolores whose patience and understanding assured the completion of this work.

---

**TABLE OF CONTENTS**

<b>ABSTRACT</b>	ii
<b>ACKNOWLEDGEMENTS</b>	iii
<b>TABLE OF CONTENTS</b>	iv
<b>LIST OF TABLES</b>	v
<b>LIST OF FIGURES</b>	vi
<b>INTRODUCTION</b>	1
<b>THEORY</b>	4
<b>EXPERIMENTAL</b>	8
<b>DISCUSSION</b>	13
<b>Water</b>	11
<b>Addition of cations</b>	29
<b>Addition of anions</b>	48
<b>CONCLUSION</b>	111
<b>REFERENCES</b>	115

LIST OF TABLES

1	Aqueous solutions studied	10
2	Low frequency spectral data for water	14
3	Spectral data for saturated alkali and alkaline earth chloride solutions	38
4	Ratio of scattering intensities for aqueous chloride solutions	39
5	$I_{ISO}$ for saturated aqueous alkali and alkaline earth chloride solutions	42
6	$I_{VH}$ data for $K_2CO_3$ (aq)	48
7	Spectral data for aqueous halides	53
8	$I_{VV}$ data for aqueous hydroxides	61

LIST OF FIGURES

Fig. 1.	$I_{VV}$ and $I_{VH}$ spectra of $H_2O$ .	13
Fig. 2.	$R(\omega)$ spectra for $H_2O$ .	16
Fig. 3.	$I(\omega)$ spectra of $H_2^{18}O$ .	19
Fig. 4.	$R(\omega)$ spectra for $H_2^{18}O$ .	21
Fig. 5.	$I(\omega)$ spectra of $D_2O$ .	23
Fig. 6.	$-R_p(\omega)$ spectra for $D_2O$ .	25
Fig. 7.	Comparison of the $R(\omega)$ spectra for $H_2O$ from $I_{VH}$ data with $\alpha(\omega)$ for $H_2O$ from refractive index infrared studies.	28
Fig. 8.	$I_{VV}$ Raman spectral data for saturated solutions of $CaCl_2$ , $MgCl_2$ , $LiCl$ , and that of water.	31
Fig. 9.	$I_{VH}$ Raman spectral data for saturated solutions of $CaCl_2$ , $MgCl_2$ , $LiCl$ , and for water intensity scaled with a $0.5M$ $KNO_3$ internal standard.	33
Fig. 10.	$R(\omega)$ spectra from transformed $I_{VV}$ spectral data for saturated aqueous chloride solutions.	35
Fig. 11.	$R(\omega)$ spectra from transformed $I_{VH}$ spectral data for saturated aqueous chloride solutions.	37
Fig. 12.	$R(\omega)$ spectra for saturated $MgCl_2$ (aq).	41
Fig. 13.	$R(\omega)$ spectra for saturated $LiCl$ (aq).	45

Fig. 14.	$R(\omega)$ spectra for saturated $\text{CaCl}_2$ (aq).	47
Fig. 15.	$R(\omega)$ spectra of $1 \text{ mol L}^{-1}$ and saturated aqueous $\text{K}_2\text{CO}_3$ solutions from $0 - 1000 \text{ cm}^{-1}$	50
Fig. 16.	$R(\omega)$ spectra of $1 \text{ mol L}^{-1}$ and saturated aqueous $\text{K}_2\text{CO}_3$ solutions normalized to the $\text{O} \cdots \text{H}-\text{O}$ stretching mode of water.	52
Fig. 17.	$R(\omega)$ spectra for saturated aqueous $\text{NaCl}$ .	55
Fig. 18.	$R(\omega)$ spectra of saturated aqueous $\text{KCl}$ .	57
Fig. 19.	$R(\omega)$ spectra of saturated aqueous $\text{KF}$ .	60
Fig. 20.	$I_{\text{VV}}$ and $I_{\text{VH}}$ spectra for $2.5 \text{ mol L}^{-1}$ $\text{LiOH}$ (aq).	63
Fig. 21.	$I_{\text{VV}}$ and $I_{\text{VH}}$ spectra for $3.95 \text{ mol L}^{-1}$ $\text{LiOH}$ (aq).	65
Fig. 22.	$I_{\text{VV}}$ and $I_{\text{VH}}$ spectra for $10 \text{ mol L}^{-1}$ $\text{NaOH}$ (aq).	67
Fig. 23.	$I_{\text{VV}}$ and $I_{\text{VH}}$ spectra for $11.5 \text{ mol L}^{-1}$ $\text{KOH}$ (aq).	69
Fig. 24.	$I_{\text{VV}}$ and $I_{\text{VH}}$ spectra for $5.9 \text{ mol L}^{-1}$ $\text{RbOH}$ (aq).	71
Fig. 25.	$I_{\text{VV}}$ and $I_{\text{VH}}$ spectra for $8.6 \text{ mol L}^{-1}$ $\text{CsOH}$ (aq).	73
Fig. 26.	$I_{\text{VV}}$ and $I_{\text{VH}}$ spectra for $10 \text{ mol L}^{-1}$ $\text{NaOD}$ (aq).	75
Fig. 27.	$R(\omega)$ spectra for $10 \text{ mol L}^{-1}$ $\text{NaOH}$ (aq).	78
Fig. 28.	$R(\omega)$ spectra for $11.5 \text{ mol L}^{-1}$ $\text{KOH}$ (aq).	80
Fig. 29.	$R(\omega)$ spectra for $5.9 \text{ mol L}^{-1}$ $\text{RbOH}$ (aq).	82

Fig. 30.	$R(\omega)$ spectra from $I_{\text{RO}}$ data for 10 mol L <sup>-1</sup> NaOH, 11.5 mol L <sup>-1</sup> KOH and 5.9 mol L <sup>-1</sup> RbOH.	84
Fig. 31.	$R(\omega)$ spectra for 8.6 mol L <sup>-1</sup> CsOH (aq).	86
Fig. 32.	$R(\omega)$ spectra for 2.5 mol L <sup>-1</sup> LiOH (aq).	89
Fig. 33.	$R(\omega)$ spectra for 3.95 mol L <sup>-1</sup> LiOH (aq).	91
Fig. 34.	Comparison of the $R(\omega)$ isotropic components for 2.5 mol L <sup>-1</sup> and 3.95 mol L <sup>-1</sup> LiOH (aq).	93
Fig. 35.	$R(\omega)$ spectra for 10 mol L <sup>-1</sup> NaOD in D <sub>2</sub> O.	96
Fig. 36.	$R(\omega)$ spectra for 10 mol L <sup>-1</sup> NaOD in D <sub>2</sub> O showing increasing background intensity from fluorescing impurities.	98
Fig. 37.	$I_{\text{VV}}$ spectrum to 4000 cm <sup>-1</sup> for 5 mol L <sup>-1</sup> NaOH (aq).	100
Fig. 38.	$I_{\text{VV}}$ spectrum to 4000 cm <sup>-1</sup> for 10 mol L <sup>-1</sup> NaOH (aq).	102
Fig. 39.	$R(\omega)$ spectrum to 4000 cm <sup>-1</sup> of $I_{\text{VV}}$ data for 5 mol L <sup>-1</sup> NaOH (aq).	104
Fig. 40.	$R(\omega)$ spectrum to 4000 cm <sup>-1</sup> of $I_{\text{VV}}$ data for 10 mol L <sup>-1</sup> NaOH (aq).	106
Fig. 41.	$I_{\text{VV}}$ spectrum of NaClO <sub>4</sub> /NaOH (5 mol L <sup>-1</sup> in each) to 4000 cm <sup>-1</sup> .	108
Fig. 42.	$R(\omega)$ spectrum of NaClO <sub>4</sub> /NaOH (5 mol L <sup>-1</sup> in each) to 4000 cm <sup>-1</sup> taken from $I_{\text{VV}}$ data.	110



Fig. 43.

$R(\omega)$  spectra of 5 mol L<sup>-1</sup> NaOH, 10 mol L<sup>-1</sup> NaOH and NaClO<sub>4</sub>/NaOH (5 mol L<sup>-1</sup> in each) taken from  $I_W$  data and normalized to the OH<sup>-</sup> intramolecular stretch at 3606 cm<sup>-1</sup>.

113

## INTRODUCTION

Vibrational spectroscopy allows one to develop a picture of a system of molecular units with intermolecular interactions. Peaks arising from internal modes of a molecule help to identify the molecular species present while changes in the peak maximum,  $\nu_{\max}$ , and full width at half height,  $\Gamma$ , and low frequency scattering yield information on forces acting between the species. When applied to water, a large amount of spectral activity is observed not all of which is easily translated to a simple molecular picture. In fact "H<sub>2</sub>O" is anything but simple. The relationship between the Raman spectrum and the structure of water and aqueous solutions is not well understood. Improved definition of the bands present in the Raman spectrum is required and can be achieved through high quality multi-scan recording of the spectral data.

Most of the work on water and aqueous salt systems has been reviewed by Walrafen [1] and has been updated to about 1977 [2,3]. The original work of Walrafen [4] covered a broad base for the Raman techniques available at the time and much of the work since has confirmed his experimental findings. The low frequency intermolecular region is considered to extend from 0 - 1000  $\text{cm}^{-1}$  for H<sub>2</sub>O and is subdivided into two regions. The librational region extends outward from 350  $\text{cm}^{-1}$  and this is supported by a local structure model of a C<sub>2v</sub> 5 molecule unit moving in a cage of nearest neighbors [5]. This C<sub>2v</sub> unit is believed to be analogous to the  $i_h$  ice structure for those waters fully hydrogen bonded. The librational region is yet to be fitted with any great certainty, but it is believed to be comprised of three peaks. The region below 350  $\text{cm}^{-1}$  is thought to be of a translational nature. Problems arise in the assignment of frequencies to bands in this region due to the large contribution of

scattered light from the wing of the Rayleigh peak to the Raman spectrum. Assignment of one band ranges from  $170 \text{ cm}^{-1}$  [6] to  $191 \text{ cm}^{-1}$  [7] for the  $\text{O} \cdots \text{H}-\text{O}$  stretch. A similar band has been reported in the IR at  $190 \text{ cm}^{-1}$  and at  $22 \text{ meV}$  [8] and  $8.4 \text{ \AA}^{-1}$  [9] for inelastic neutron scattering and neutron diffraction studies respectively. Discrepancies are also apparent in the reported Raman frequencies for  $\text{D}_2\text{O}$  -  $175 \text{ cm}^{-1}$  [4],  $191 \text{ cm}^{-1}$  [7], and  $180 \text{ cm}^{-1}$  [10] - and for  $\text{H}_2^{18}\text{O}$  -  $181 \text{ cm}^{-1}$  [7] and  $170 \text{ cm}^{-1}$  [10]. A weaker  $\text{O} \cdots \text{H}-\text{O}$  bending mode has been assigned a frequency of  $60 \text{ cm}^{-1}$  for  $\text{H}_2\text{O}$ ,  $\text{H}_2^{18}\text{O}$  and  $\text{D}_2\text{O}$  [10]. The intensity of both regions drops with increasing temperature [1,4,7] while the Rayleigh scattering increases [11] faster than would be predicted by collision induced polarizability theory - phenomena which show a breakdown in the water structure.

Various effects on the Raman spectrum of water have been noticed when ionic salts are added. Addition of anions, such as bromides and chlorides, reportedly lower the intensity of the translational region while raising the intensity of the librational region [4]. Similar changes have been observed in the IR [12] and Rayleigh scattering [13] and have been interpreted as anion hydrate contribution to the librational region spectrum plus a loss of water-water interaction (structure breaking) [4,11,14,15]. Perchlorate, except for  $\text{HClO}_4$ , has been classified as a structure breaker in water [7,14] virtually wiping out the  $\text{O} \cdots \text{H}-\text{O}$   $190 \text{ cm}^{-1}$  stretch in the Raman spectrum. The presence of an isosbestic point in the infrared librational region of water has been interpreted as evidence for an equilibrium between waters of hydration and bulk water ( $\text{C}_{2V}$  molecular unit) [16] but no evidence of a water-perchlorate hydrogen bond stretch was found in the translational vibrational spectra because of the weak bond that

forms between  $\text{ClO}_4^-$  and  $\text{H}_2\text{O}$  [17,18]. Other anions such as  $\text{F}^-$  and  $\text{OH}^-$  are considered structure enhancing in water. Both IR [19] and Raman [7] studies indicate an increased intensity and  $\nu_{\text{max}}$  for the  $\text{O}\cdots\text{H}-\text{O}$  stretch band with  $\text{F}^-$  addition, and recent X-ray [20] and SCF calculations with correlations for configurational interactions with single and double substitutions [21] show a symmetric  $\text{H}_3\text{O}_2^-$  ion formed from an  $\text{OH}^-\cdots\text{H}_2\text{O}$  interaction.

Information concerning cation effects on the low frequency water spectrum is scarce and such effects are generally considered to be small even though new peaks due to metal-oxygen vibrations of hydrated cations are often observed [2]. A Raman study of aqueous lithium halides [12] reported that in dilute solutions a tetrahedral  $\text{Li}(\text{H}_2\text{O})_4^+$  species exists with the  $A_1$  mode at  $440\text{ cm}^{-1}$  but that at saturation levels ion aggregates or solvent separated ion pairs form.

Refractive index studies suggest that most of the low frequency spectral changes of water in aqueous salt solutions are due to the effects of ions on  $\text{H}_2\text{O} - \text{H}_2\text{O}$  interactions [19], although recent Raman studies show that intense scattering also arises from reorientations of anisotropic ions [7]. Newer Rayleigh scattering studies [22] also showed the contribution from anisotropic ions. Poor correlation between solution entropies for polyatomic ions and shifts for the first moment of the IR librational bands for their aqueous solutions were interpreted to indicate that anion reorientation is contributing to the solution entropy [14]. These reorientational bands of anisotropic molecules and ions are easily seen in the Raman spectrum when the spectrum is recast in a density of states format  $R(\omega)$ .

This study begins with a look at the Raman spectrum of water and its isotopic analogues  $\text{D}_2\text{O}$  and  $\text{H}_2^{18}\text{O}$  in an  $R(\omega)$  format in the hope that a

more precise assignment of the low frequency bands may be obtained. Isotope shifts observed for the O...H-O stretch show that hydrogen-oxygen stretching is different for the two oxygens involved. Raman spectral evidence for cation effects on the low frequency spectrum of aqueous solutions is reported for LiCl, MgCl<sub>2</sub> and CaCl<sub>2</sub>. A polarized band is observed in aqueous LiCl at 384 cm<sup>-1</sup> and is similar to the symmetric stretch for the hexahydrated magnesium ion which appears at 359 cm<sup>-1</sup>. No evidence of such a band is seen for CaCl<sub>2</sub>. Strong anion-water interactions are reported for F<sup>-</sup> and OH<sup>-</sup> and a polarized band appearing in the Raman spectra of their aqueous solutions is assigned to an O-H...X<sup>-</sup> symmetric stretch. The presence of the structure breaking ClO<sub>4</sub><sup>-</sup> ion is shown to disrupt both water-water interactions and hydroxide-water interactions. The polarizability anisotropy of the CO<sub>3</sub><sup>2-</sup> ion gives rise to a reorientational band in the depolarized spectra of its aqueous solutions. The frequency of this band is very close to that for NO<sub>3</sub><sup>-</sup> [7].

The spectra for all of the solutions studied were cast in an  $R(\omega)$  format to obtain more detail from the low frequency Raman spectra. No attempt is made to test the relationship of  $R(\omega)$  to  $\alpha(\omega)$  from the IR but a comparison of  $R(\omega)$  for the depolarized spectrum of water and  $\alpha(\omega)$  for water show similarities between the two spectra.

#### THEORY

The primary problem in the study of low frequency Raman scattering is correcting for the contribution from Rayleigh scattering. Molecular processes giving rise to bands in this region are generally of a weak nature and arise from such actions as reorientational motions of molecules with permanent anisotropy or collision induced anisotropy, intermolecular vibrations of hydrogen bonded species and, vibrations of molecules with

weak bonds or containing heavy atoms. Difference bands may also be present in this region. The difference in intensity between the Rayleigh scattered light and the low frequency Raman scattered light may be so great that the Raman band only appears as a deformation of the Rayleigh wing. Determination of band shapes and positions of the low frequency modes requires removal of (or accounting for) the contribution of the Rayleigh wing to the spectrum.

Some understanding of the functional form of the scattering in this region has been found in the study of temperature effects on the scattering of some glasses. Stolen [23] and Hass [24] have reported a spectral dependence for glasses in the low frequency Raman of  $|1+n(\omega)|$  where

$$n(\omega) = \left[ e^{-\hbar\omega/2\pi kT} - 1 \right]^{-1}$$

That is to say, much of the shape of the  $\omega=0$  peak is due to a thermal population factor. When the spectra are corrected for the thermal factor, the spectra appear in the form of a vibrational density of states. Hass has shown that, when a density of states spectrum is recast in an  $I(\omega)$  form at different temperatures, the experimental spectra match the calculated spectra very closely. Shuker and Gammon [25] have shown the dependence of viscous liquids on the population factor and a common frequency factor. Under the assumption that the scattering is due to vibrations and the modes have short lived correlation functions, the scattering is first order, disorder allowed [26]. The result is

$$I(\omega) = \sum_b C_b (1/\omega) |1+n(\omega)| g_b(\omega)$$

where  $C_b$  is the coupling constant over the vibration at band  $b$  and  $g_b(\omega)$  is the density of states of vibration  $b$ . Hence to cast the  $I(\omega)$  spectrum in a form of  $g_b(\omega)$ , the spectrum can be multiplied by the factor

$\omega/[1+n(\omega)]$ . Recently it has been shown that the coupling constant may vary across the band [27] in which case the application of this function may not be a true representation of the density of states.

Lund et al. [10, 28] have arrived at the same function from another approach. These workers derive a function,  $R(\omega)$ , which is proportional to the energy absorbed in a scattering process.

$$R(\omega) = \omega [S^>(\omega) - S^<(\omega)].$$

Here  $S^>(\omega)$  and  $S^<(\omega)$  refer respectively to the Stokes and anti-Stokes scattered light intensities. The mean scattered light intensity  $S(\omega)$  is given by  $S(\omega) = 1/2 [S^>(\omega) + S^<(\omega)]$  and is a function of the molecular polarizabilities

$$S(\omega) = \int_{-\infty}^{\infty} e^{-i\omega t} \langle \alpha^2(0) \alpha(t) \rangle dt$$

where  $I_{if} = (1/4) k_f^4 / 16\pi^2 R^2 \epsilon_0^2 (1/2\pi) S(\omega)$  is the intensity of scattered light of frequency  $\omega = \omega_f - \omega_i$  and subscripts  $i$  and  $f$  refer to the initial and final states of the transition. From the principle of balanced states,

$$\left[ \frac{S^<(\omega)}{S^>(\omega)} \right] = e^{-\frac{h\omega}{2kT}}$$

and

$$R(\omega) = S^>(\omega) \omega [1 - e^{-h\omega/2kT}].$$

It can be easily shown that  $[1 - e^{-h\omega/2kT}] = [1+n(\omega)]$ . Lund goes a step further in showing the relationship of  $R(\omega)$  to  $\alpha(\omega)$ , the IR absorption coefficient. In the process he has assumed that in the far IR for most liquids  $\alpha(\omega)$  is proportional to  $\omega e'$ . This approximation results in:

$$\alpha(\omega) = \omega \tanh \left[ \frac{h\omega}{4kT} \right] \int_{-\infty}^{\infty} e^{-i\omega t} \langle \vec{u}(0) \cdot \vec{u}(t) \rangle dt$$

where  $\langle \vec{u}(0) \cdot \vec{u}(t) \rangle$  is the dipole moment correlation function. Since  $S(\omega) = 1/2 [S^>(\omega) + S^<(\omega)]$  then

$$S^>(\omega) = \frac{2S(\omega)}{[1 + e^{-h\omega/2\pi kT}]}$$

and

$$R(\omega) = 2S(\omega)\omega \left[ \frac{1 - e^{-\frac{h\omega}{2\pi kT}}}{1 + e^{-\frac{h\omega}{2\pi kT}}} \right]$$

which is easily shown to be:

$$R(\omega) = 2\omega \tanh\left[\frac{h\omega}{4\pi kT}\right] \int_{-\infty}^{\infty} e^{-i\omega t} \langle \alpha(0)\alpha(t) \rangle dt.$$

This is strikingly similar to the formula for the infrared absorption coefficient except for the dependence of the two processes on different selection rules. In the high temperature low frequency limit the  $R(\omega)$  function approaches the classical second moment  $M_2$ . The second moment has its roots in the 'Method of Moments' approach to creating a Heisenberg picture from the energy domain (i.e. the Fourier transform of the energy spectrum). The second moment is the Fourier transform of the second time derivative of the rotational correlation function.

$$G_r(t) = \langle 1/2 \left[ 3 [\vec{u}(0) \cdot \vec{u}(t)]^2 - 1 \right] \rangle$$

[29].

$$M_2 = \frac{\int_{-\infty}^{\infty} I(\omega)\omega^2 d\omega}{\int_{-\infty}^{\infty} I(\omega) d\omega} = -FT \left[ \frac{d^2 G_r(t)}{dt^2} \right]$$

Although the second moment has been used to approximate the  $R(\omega)$  spectrum [30], it has a different meaning in its derivation and should not be equated rigidly in its interpretation.

Discrepancies exist in the literature [10,30,28] as to which function (tanh or exponential) should be applied. Since most Raman experiments only measure the Stokes shifts, the function to be applied should be the



exponential form as this will relate  $S^>(\omega)$  to  $R(\omega)$  directly. In order to use the hyperbolic tan function both Stokes and anti-Stokes shifts must be collected and one added to the other.

The function one applies depends on the ultimate goal. If comparison with the IR absorption coefficients is to be performed, the density of states function or  $R(\omega)$  must be used provided of course there is a possibility of comparison with the IR (ie.  $\epsilon'' = \epsilon''(\omega)/n(\omega)c$  where  $n(\omega)$  is the index of refraction or  $K_{\omega} = 1$ ). In the case where no comparison is necessary, either of the functions (hyperbolic tan, exponential, or classical second moment) will enable easier viewing of the low frequency Raman as they virtually remove the effect of the Rayleigh line. In the present study, the exponential form of the  $R(\omega)$  was used.

One practical problem with any of these approaches to data treatment is the apparent increase of the noise with increasing frequency. This can be minimized through repetitive scans and signal averaging. The relative increase in noise is not unexpected as the functions are designed to study the  $\omega=0$  band and this increase represents the deterioration of the S/N ratio of the  $\omega=0$  band with increasing  $\omega$ .

#### EXPERIMENTAL

In order to study the effects of ions on the low frequency region of water in the Raman spectrum, it is necessary to maintain high purity and homogeneity in the solutions used. Reagent grade salts were purified with activated charcoal in distilled water to remove any fluorescing materials. The charcoal was removed by filtration through fine frits and the salts recrystallized. The solutions were then prepared by dissolving the required amounts of the salts in doubly distilled water. For the saturated solutions, the salts were added in excess and equilibrated for one week. Solutions

were filtered through fine frits to remove any particles which might give rise to Tyndall scattering. The sample tubes were protected from solvent evaporation with Parafilm. In the case of the isotopic waters, treatment was excused on the grounds that the solutions were already of relatively high purity -  $D_2O$ , 99.8% D and  $H_2^{18}O$ , 99%  $^{18}O$  - and on the high cost due to loss of solution that may occur during treatment. The aqueous solutions appear in Table 1. In addition to these solutions, spectrograde methanol and methanol 5.1M in NaOH were prepared. NaOH and 1:1 NaOH:KOH melts were also prepared for comparison.

The spectra were recorded at 298 K on a CODERG PHO Raman spectrometer using the 488 nm line of a CONTROL model 553A argon ion laser. The laser power varied between 150 mW and 600 mW c.w. depending on the scattering ability of the sample. The incident light was vertically polarized and the scattered light, collected at right angles to the incident beam, was analyzed through a vertically or horizontally aligned polaroid film to give  $I_{VV}$  or  $I_{VH}$  polarizations. A quarter waveplate was employed to overcome the instrument polarization preference. The sample tubes were masked at the entry and exit points of the laser beam to minimize scattering from the glass. The slit widths for the double monochromator were set at  $2 \text{ cm}^{-1}$ . The PMT was cooled to  $-20^\circ\text{C}$  and signals collected via photon counting. The scan rate was  $50 \text{ cm}^{-1}/\text{min}$ . and the counts were one point per wavenumber for scans to  $1000 \text{ cm}^{-1}$  and two points per wavenumber for scans to  $400 \text{ cm}^{-1}$ . The spectra were wavenumber calibrated with the  $351.64 \text{ cm}^{-1}$  plasma line. Spectra were collected ten times in both  $I_{VV}$  and  $I_{VH}$  orientations and the digital output recorded on disk at the M.U.N. Computer Services VAX - 11/780. Data processing involved signal averaging to produce intensity and density of

Table 1

Aqueous solutions studied

Solution	Concentration
LiCl (Sat.)	15.03m
MgCl <sub>2</sub> (Sat.)	5.70m
CaCl <sub>2</sub> (Sat.)	6.71m
KF (Sat.)	15.69m
KCl (Sat.)	4.85m
NaCl (Sat.)	6.11m
K <sub>2</sub> CO <sub>3</sub> (Sat.)	8.10m
K <sub>2</sub> CO <sub>3</sub>	1M
LiOH	2.5M (0.010M in carbonate)
KOH	11.5M (0.031M in carbonate)
NaOH	10M (0.074M in carbonate)
RbOH	5.9M (0.25M in carbonate)
CaOH	8.6M (2.58M in carbonate)
NaOH + NaClO <sub>4</sub>	5M in each
NaOD in D <sub>2</sub> O	10M

states spectra for both orientations of the scattered light. The resulting spectra were then plotted on a TEKTRONIX 4662 digital interactive plotter with the aid of a TEKTRONIX 4051 graphics terminal. Further data treatment was applied to the pure water and to the saturated lithium, calcium,

and magnesium chloride solutions to provide a relative intensity comparison. Intensity spectra were first calibrated to the integrated absorption of the  $\nu_2$  H-O-H bending region of the water. Since the bending region of the water is not constant with concentration [31,32], a second set of solutions was prepared and the  $\nu_2$  water region was further calibrated with the symmetric stretch region of the nitrate ion (linearly concentration dependent) by the addition of 0.5M Potassium Nitrate as an internal standard. The result was a set of scaled intensity spectra for the low frequency region without the introduction of a material which could itself contribute to the low frequency scattering. Finally the  $R(\omega)$  spectra were scaled to have the same ratio of integrations as was apparent in the intensity spectra over a region where the spectra changed little with frequency. Subtraction files were created for some spectra by subtracting the  $I_{VH}$  data from the corresponding  $I_{VV}$  data to give the isotropic Raman spectrum  $I_{ISO} = I_{VV} - 4/3 I_{VH}$ .

## DISCUSSION

### Water

The earlier work [4] on the intermolecular vibration region of water has not been improved much even in recent years. This is due to attempts to fit this low intensity region in the  $I(\omega)$  format. The intermolecular Raman spectrum of water is shown in Fig. 1. In the range above  $300 \text{ cm}^{-1}$  there is a broad weak envelope, the number of components of which are not visibly evident. Below  $300 \text{ cm}^{-1}$  there is a broad peak at about  $190 \text{ cm}^{-1}$  and evidence of some intensity at about  $70 \text{ cm}^{-1}$ . Below this frequency, information becomes lost as the intensity of the Rayleigh scatter becomes more intense. The same features are present in both the polar-

7


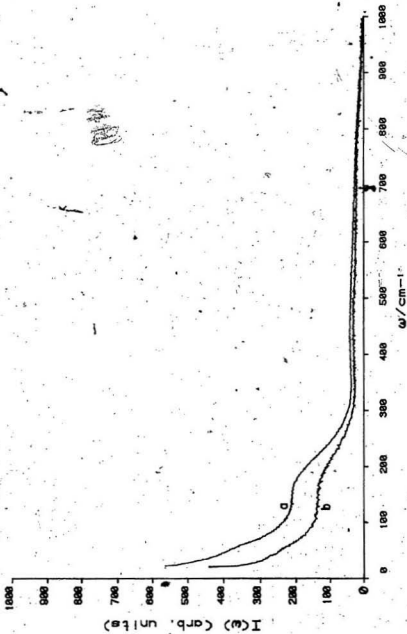


Fig. 1.  $I_{VV}$  (a) and  $I_{VH}$  (b) spectra of  $H_2O$ . Weak features due to translations and librations of water are observed from  $100\text{ cm}^{-1}$  to  $1000\text{ cm}^{-1}$ . A mostly depolarized nature is exhibited in the spectra:



ized and depolarized spectra. It is unclear as to whether any polarized Raman components are present since the drop in the Rayleigh scatter is so large when the polaroid analyzer is reoriented.

The spectrum of water in an  $R(\omega)$  format appears in Fig. 2 and the data for  $H_2O$ ,  $H_2^{18}O$  and  $D_2O$  is given in Table 2.

Table 2  
Low frequency spectral data for water  
 $cm^{-1}$

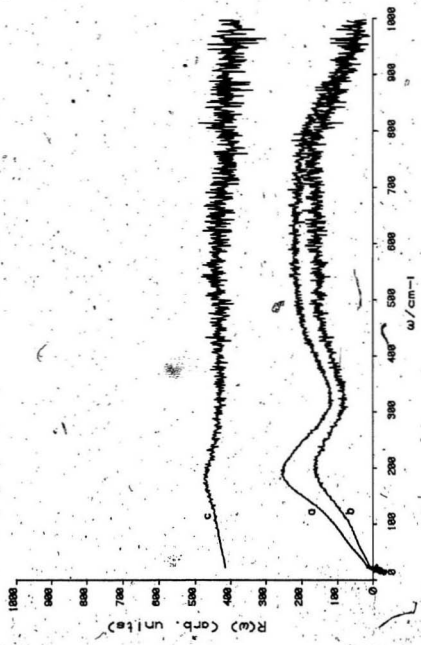
		$\nu_{O-H-O}$ bend	$\nu_{O-H-O}$ str	$\nu_{lib}$
$H_2O$	I <sub>W</sub>	66 (68)	182 (252)	250 - 1000 (220) at 550
	I <sub>VH</sub>	66 (40)	186 (162)	250 - 1000 (156) at 550
$H_2^{18}O$	I <sub>W</sub>	55 (215)	175 (482)	250 - 1000 (382) at 550
	I <sub>VH</sub>	55 (170)	178 (408)	250 - 1000 (358) at 550
$D_2O$	I <sub>W</sub>	55 (187)	186 (485)	- 800
	I <sub>VH</sub>	55 (143)	186 (376)	- 800

Brackets contain relative intensities.

A multi-component region exists between  $300\text{ cm}^{-1}$  and  $1000\text{ cm}^{-1}$ . No attempt has been made in this work to analyze the number of components in this region, but the presence of two or more bands is a necessity and due to the relatively steep slope on the high frequency wing it is probable that three peaks would be required. A fit of this region [33] from the

Fig. 2.  $R(\omega)$  spectra for  $H_2O$ . Transformed  $I_{VV}$  data (a) and  $I_{VH}$  data (b) show the same band features as in Fig. 1 but with greater definition. The hydrogen bond stretch is seen at  $192\text{ cm}^{-1}$  in the polarized spectrum and a weaker depolarized  $O\cdots H-O$  bending mode is observed at  $66\text{ cm}^{-1}$ . The band at  $192\text{ cm}^{-1}$  is slightly polarized as demonstrated by the isotropic spectrum (c).





$I(\omega)$  format has incorporated three bands at 425, 550, and 740  $\text{cm}^{-1}$  with half-widths ranging between 200 and 250  $\text{cm}^{-1}$ . Below 300  $\text{cm}^{-1}$  the bands in the  $R(\omega)$  (Fig. 2) stand out more so than in the  $I(\omega)$  format. The band assigned to the hydrogen bond stretching mode [4,6,7,10] appears at 192  $\text{cm}^{-1}$  and the  $\text{O}\cdots\text{H}-\text{O}$  bending mode occurs at about 66  $\text{cm}^{-1}$ . No peaks are visible below 50  $\text{cm}^{-1}$ . The subtraction spectrum shows a slight polarization characteristic for the 192  $\text{cm}^{-1}$  band; but the maximum occurs at about 178  $\text{cm}^{-1}$ . The depolarized spectrum shows the maximum at a slightly higher frequency than does the polarized spectrum. The reason for this difference is unclear but it might be due to the influence of stray Rayleigh scattered light.

The  $I(\omega)$  and  $R(\omega)$  spectra for  $\text{H}_2^{18}\text{O}$  and  $\text{D}_2\text{O}$  are shown in Figs. 3 to 6. Comparison of the frequency range between 300  $\text{cm}^{-1}$  and 1000  $\text{cm}^{-1}$  for  $\text{H}_2\text{O}$  and  $\text{H}_2^{18}\text{O}$  reveals little difference while the envelope for  $\text{D}_2\text{O}$  is shifted to lower frequencies. This independence of mass for the central atom and large dependence on mass for the attached atoms leads to the conclusion that the modes are librational in nature and confirms the earlier assignment of this region to librations of the water species [4]. The assignment of the 192  $\text{cm}^{-1}$  band of water to  $\text{O}\cdots\text{H}-\text{O}$  stretching is supported by the frequency shift to 175  $\text{cm}^{-1}$  for  $\text{H}_2^{18}\text{O}$  and 186  $\text{cm}^{-1}$  for  $\text{D}_2\text{O}$ . The 66  $\text{cm}^{-1}$  band drops in frequency to 55  $\text{cm}^{-1}$  for both  $\text{H}_2^{18}\text{O}$  and  $\text{D}_2\text{O}$ . Pure translational modes should exhibit frequency shifts of the ratio  $(18/20)^{1/2} = 0.9487$  for both  $\text{D}_2\text{O}$  and  $\text{H}_2^{18}\text{O}$ . The shifts for the stretching modes of  $\text{H}_2^{18}\text{O}$  and  $\text{D}_2\text{O}$  are 0.9211 and 0.9474 respectively. An independence of the  $\text{O}\cdots\text{H}-\text{O}$  stretching mode with deuteration was reported in previous studies [4,7,10]. The present work reveals only a slight shift in this mode for  $\text{D}_2\text{O}$ . There is however a greater uncertainty

Fig. 3.  $I(\omega)$  spectra of  $H_2^{18}O$ .  $I_{\text{W}}$  (a) and  $I_{\text{VH}}$  (b).

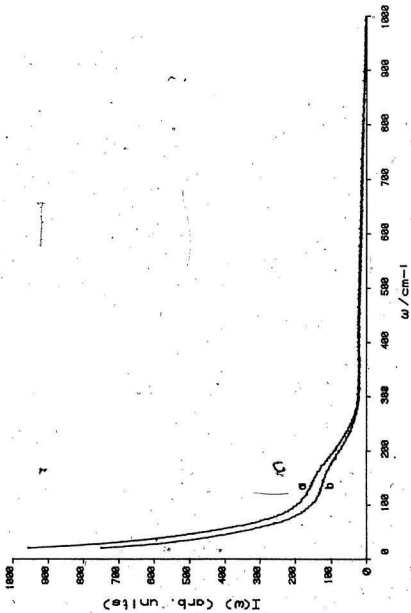


Fig. 4.  $R(\omega)$  spectra for  $H_2^{18}O$ . Transformed  $I_{VV}$  (a) and  $I_{VH}$  (b) spectra show that the  $O\cdots H-O$  stretch is slightly polarized and shifts  $17\text{ cm}^{-1}$  from that of  $H_2O$  to  $175\text{ cm}^{-1}$  confirming the assignment of this band to oxygen moving about the hydrogen [7]. The hydrogen bond bending mode is seen at  $55\text{ cm}^{-1}$ .

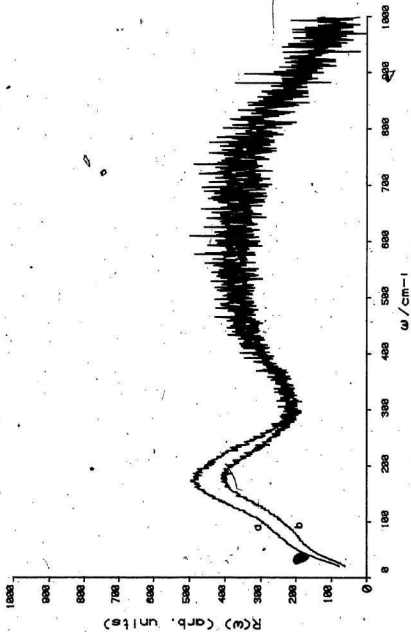
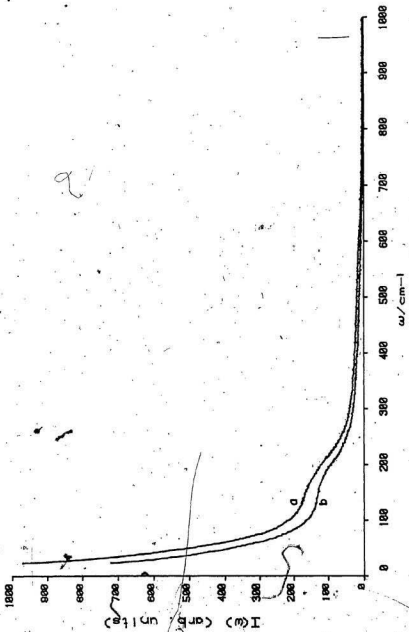


Fig. 5.  $I(\omega)$  spectra of  $D_2O$ .  $I_W$  (a) and  $I_{VH}$  (b).





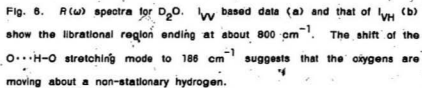
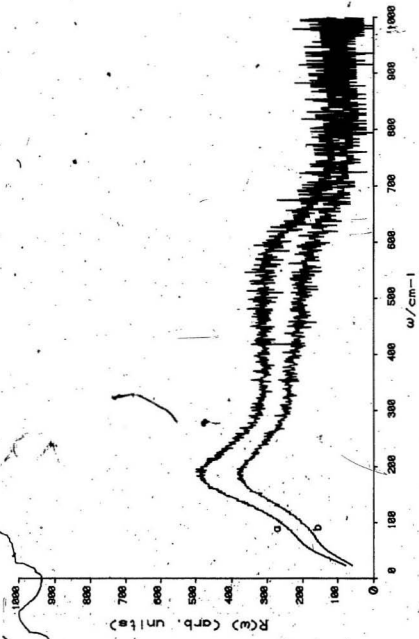


Fig. 6.  $R(\omega)$  spectra for  $D_2O$ .  $I_W$  based data (a) and that of  $I_{VH}$  (b) show the librational region ending at about  $800\text{ cm}^{-1}$ . The shift of the  $O\cdots H-O$  stretching mode to  $186\text{ cm}^{-1}$  suggests that the oxygens are moving about a non-stationary hydrogen.

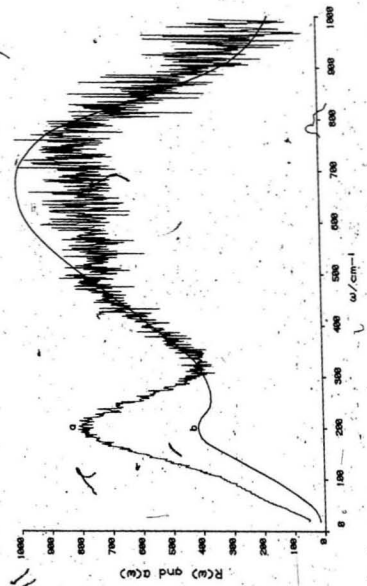


In the quote frequency ( $186 \text{ cm}^{-1}$ ) for the stretching mode because of overlap from the librational band. If the shift for the hydrogen bond stretching mode is real then the picture of two oxygens moving about the hydrogen as suggested by Brooker and Perrot [7] should be adjusted to show oxygen movement about a non-stationary hydrogen, i.e. the hydrogen remains closer to one of the oxygens, the oxygen to which it is hydrogen bonded. This would be further support for the assignment of the  $192 \text{ cm}^{-1}$  band in the Raman spectrum of water to a restricted translation of a water molecule from an intermolecular hydrogen-oxygen bond.

Moskovits and Michaellah [8] have reported a band at  $170 \text{ cm}^{-1}$  in the  $I(\omega)$  spectrum for  $\text{H}_2\text{O}$  with a shift to  $160 \text{ cm}^{-1}$  for  $\text{D}_2\text{O}$  as a restricted translation mode. They also reported this band to be depolarized, the bands of the librational region to be weakly polarized, and the presence of a weak slightly polarized band at  $290 \text{ cm}^{-1}$ . No support for these findings were observed in the present study.

The comparison of the  $R(\omega)$  depolarized spectrum of water and IR absorption coefficients for water, taken from [34], is presented in Fig. 7. It is apparent that the two have some similar features. Librations cover the same region and the contour of the wings of the envelopes are roughly the same. Deviation in the contours occur between  $500$  and  $700 \text{ cm}^{-1}$  and is to be expected as the different selection rules will cause certain modes to be inactive or active to different extents. In the translation region, the peak maxima positions almost coincide. The  $66 \text{ cm}^{-1}$  band is not evident from the IR data shown. The overlay of the wing intensities in the libration region is purely accidental as no scale matching was performed. Still, the plot does show some support for Lund's definition of  $R(\omega)$  [10,28].

Fig. 7. Comparison of (a) the  $R(\omega)$  spectra for  $H_2O$  from  $I_{VH}$  data with (b)  $\alpha(\omega)$  for  $H_2O$  from refractive index infrared studies [34].



#### Addition of cations

It has been previously shown that additions of ions to water causes changes in the infrared contour of the  $20 - 1000 \text{ cm}^{-1}$  region [14, 16, 19]. Various ions are able to enhance or reduce the intensity in certain regions. Others still, show contributions from the ions themselves. In the Raman it has been reported that anionic species cause measurable enhancement of the intensity of the librational region [4]. However, in this study, it will be shown that the addition of anions to water can also alter the spectra of the region below  $300 \text{ cm}^{-1}$  and in some cases contribute bands which are due to the reorientations of the anion itself. The effects on the spectrum of water from the addition of cations are reported as being very weak and to date are unavailable. The  $I(\omega)$  Raman spectra for water and saturated aqueous solutions of  $\text{CaCl}_2$ ,  $\text{MgCl}_2$  and  $\text{LiCl}$  appear in Figs. 8 and 9. These spectra were scaled with an internal reference and show the true ratio of the intensities of the scattered light. The effects of the different cations are clearly visible both with respect to the intensity and the band shape.

The  $R(\omega)$  spectra for these same solutions are presented in Figs. 10 and 11 and are summarized in Table 3. Difference spectra were constructed to reveal the  $I_{\text{ISO}}$  spectrum from  $I_{\text{VV}} - 4/3 I_{\text{VH}}$  and are included. The true meaning of the changes observed is not completely clear. What can be said to be true is that with the addition of these salts there is an increase in structure of the solution, the degree of which is not as independent of cationic species as once thought [1]. The band shape of the water libration region undergoes many changes with the various cations used, and the  $192 \text{ cm}^{-1}$  band of water is shifted to higher frequencies ( $196 \text{ cm}^{-1}$  for  $\text{CaCl}_2$ ,  $204 \text{ cm}^{-1}$  for  $\text{MgCl}_2$ , and  $193 \text{ cm}^{-1}$  for  $\text{LiCl}$ ) and

Fig. 8. Raman spectral data for saturated solutions of (a)  $\text{CaCl}_2$ , (b)  $\text{MgCl}_2$ , (c)  $\text{LiCl}$ , and that of water (d). The spectra were intensity scaled by the use of a 0.5M  $\text{KNO}_3$  internal standard.

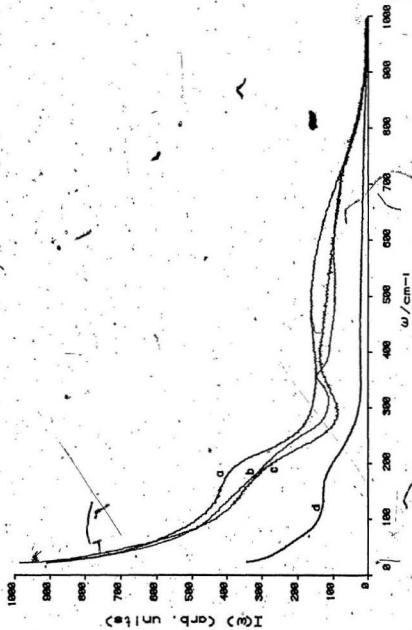
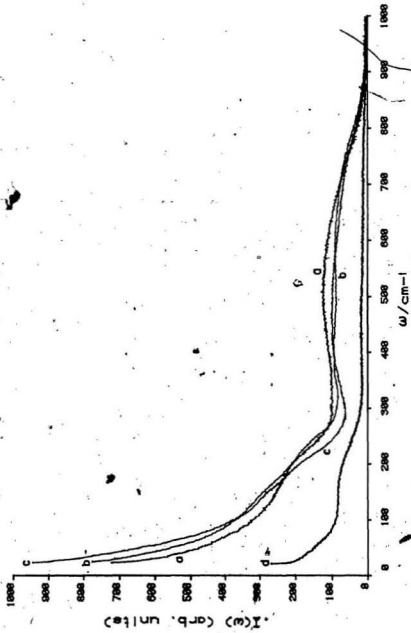




Fig. 9.  $\nu_{\text{OH}}$  Raman spectral data for saturated solutions of (a)  $\text{CaCl}_2$ , (b)  $\text{MgCl}_2$ , (c)  $\text{LiCl}$ , and for water (d) intensity scaled with a 0.5M  $\text{KNO}_3$  internal standard.







Fig. 10.  $R(\omega)$  spectra from transformed  $I_{VV}$  spectral data for saturated aqueous chloride solutions. The  $192\text{ cm}^{-1}$  band of water (d) shifts to  $196\text{ cm}^{-1}$  for  $\text{CaCl}_2$  (a),  $204\text{ cm}^{-1}$  for  $\text{MgCl}_2$  (b) and  $193\text{ cm}^{-1}$  for  $\text{LiCl}$  (c). Various changes in the contour of this region show that cation effects on the spectrum of water are real.



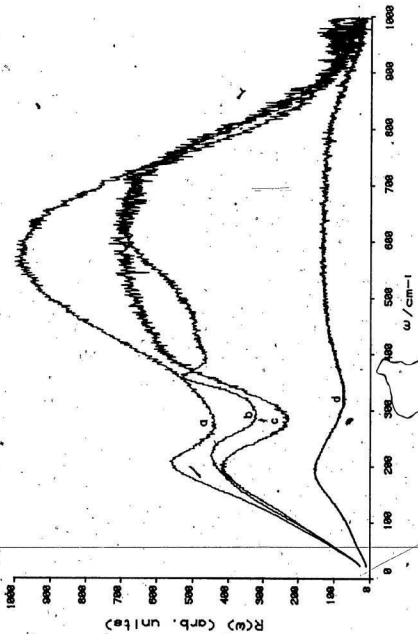


Fig. 11.  $R(\omega)$  spectra from transformed  $I_{VH}$  spectral data for saturated aqueous chloride solutions.  $\text{CaCl}_2$  (a),  $\text{MgCl}_2$  (b),  $\text{LiCl}$  (c), and  $\text{H}_2\text{O}$  (d).

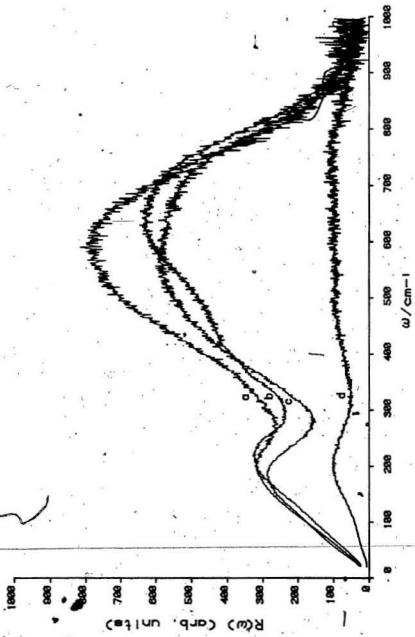


Table 3

Spectral data for saturated alkali and alkaline earth chloride solutions

		cm <sup>-1</sup>		
		$\nu_{O \cdots H-O}$ str	$\nu_{M \cdots O}$ str	$\nu_{lib}$
CaCl <sub>2</sub>	I <sub>W</sub>	196 (275)		574 (1000)
	I <sub>VH</sub>	196 (136)		593 (778)
MgCl <sub>2</sub>	I <sub>W</sub>	204 (230)	361 (159)	646 (694)
	I <sub>VH</sub>	195 (160)	361 (86)	643 (628)
LiCl	I <sub>W</sub>	193 (406)	398	597 (694)
	I <sub>VH</sub>	195 (289)		569 (586)
H <sub>2</sub> O	I <sub>W</sub>	192 (154)		550 (135)
	I <sub>VH</sub>	195 (100)		550 (94)

Brackets contain relative intensities.

Increases in intensity. This is contrary to that reported in [4] and implies some cation enhancement of the O...H-O stretch. The band at 68 cm<sup>-1</sup> in water is absent from the aqueous solution spectra. Although the ions present were chosen so as not to contribute scattering due to their own anisotropy, changes in band maxima and shape cannot be interpreted as solely due to enhanced water modes. The presence of weakly hydrated species could give rise to such changes.

Clement and Fourche have recorded total Rayleigh scattering intensity at zero frequency for these chloride solutions to 1M concentrations [15].

The ratio of intensities for their work and the present study are given in Table 4. The difference in magnitude between the two sets of data are probably due to concentration differences. The two studies show the

Table 4  
Ratio of scattering intensities for aqueous  
chloride solutions

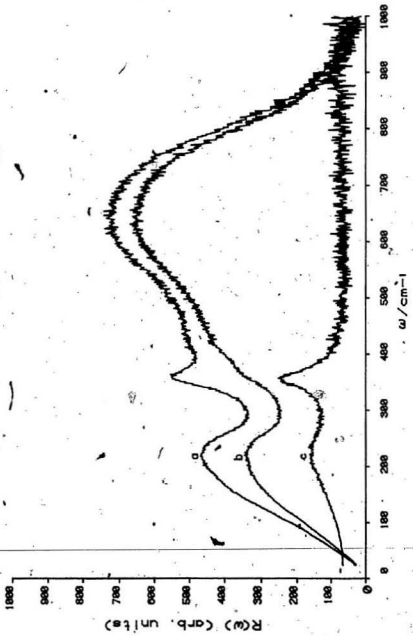
	$R(\nu)$ at $293 \text{ cm}^{-1}$	ref. [15]
$\text{H}_2\text{O}$	1.00	1.00
$\text{LiCl}$	3.03	1.16
$\text{MgCl}_2$	4.02	1.33
$\text{CaCl}_2$	4.69	>>> 1.51

scatter for  $\text{CaCl}_2 > \text{MgCl}_2 > \text{LiCl} > \text{H}_2\text{O}$  and suggest a stronger ability for solutions to scatter light with increasing size of the cation present. In fact these workers reported that the intensity from hydrated chloride is very weak and that most of the intensity of the Rayleigh scatter is a result of hydrated cations and water.

Thermodynamic calculations [35] indicate that the presence of hydrated cationic species is more probable than anionic hydrates for the same charge/mass ratio. Vibrational modes due to metal oxygen vibrations of discrete  $\text{M}(\text{H}_2\text{O})_6^{2+}$  species are well documented [2]. For  $\text{Mg}(\text{H}_2\text{O})_6^{2+}$  the  $A_{1g}$  symmetric stretch is assigned to a polarized band at  $362 \text{ cm}^{-1}$  [38]. The presence of this band and its polarized character are shown in Fig. 12 and Table 5. The difference spectrum shows the partially polarized character of the  $204 \text{ cm}^{-1}$  peak and the symmetric stretch at  $359 \text{ cm}^{-1}$ . Above this band, the difference spectrum is flat indicating the pure depolarized nature of this region. From examination of the depolarized spectrum for the  $\text{MgCl}_2$  solution, it is apparent that there exists some underlying



Fig. 12.  $R(\omega)$  spectra for saturated  $MgCl_2$  (aq). The isotropic component (c) is created from  $I_{VV}$  (a) -  $4/3 I_{VH}$  (b). Polarized peaks at  $222\text{ cm}^{-1}$  and  $359\text{ cm}^{-1}$  represent the  $O\cdots H-O$  stretching and  $M\cdots O$  stretching modes respectively in the solution. The flat portion of the difference spectrum from  $500 \rightarrow 1000\text{ cm}^{-1}$  indicates the pure depolarized nature of this region.



( Table 5  
 $I_{180}$  for saturated aqueous alkali and  
 alkaline earth chloride solutions  
 $\text{cm}^{-1}$

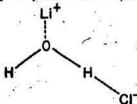
	$\nu_{O \cdots H-O}$ str	$\nu_{M \cdots O}$ str
$\text{MgCl}_2$	222 (93)	369 (165)
$\text{LiCl}$	220 (74)	364 (98)
$\text{CaCl}_2$	196 (151)	✓

Brackets contain relative intensities.

ing intensity in the  $350 - 450 \text{ cm}^{-1}$  region. Additional bands may arise from the  $E_g$  and  $F_{2g}$  Raman active internal modes of the octahedral complex. These modes are the  $\nu_2$  and  $\nu_5$  respectively and usually occur lower in frequency than the symmetric stretch. In the case of  $\text{Al}(\text{H}_2\text{O})_6^{3+}$ ,  $\nu_1$  appears at  $542 \text{ cm}^{-1}$ ,  $\nu_2$  at  $473 \text{ cm}^{-1}$  and  $\nu_5$  at  $347 \text{ cm}^{-1}$  [37]. The bands present in the depolarized spectrum of  $\text{MgCl}_2$  occur at the same frequency as the symmetric stretch and higher. The band at  $361 \text{ cm}^{-1}$  may be the residual of the symmetric stretch or  $\nu_5$  with a frequency quite close to  $\nu_1$  as  $\nu_2$  is rarely seen. The presence of depolarized intensity at  $420 \text{ cm}^{-1}$  does not fit the pattern for octahedral species and may just be due to intensity enhancement of one of the water librational components.

The  $\text{Li}^+$  ion is reported to be hydrated in aqueous solutions with a tetrahedral arrangement of water molecules for dilute solutions with an  $A_1$  mode at  $440 \text{ cm}^{-1}$ . Ion aggregates or solvent separated ion pairs in saturated solutions have been reported to give a polarized band at  $380$

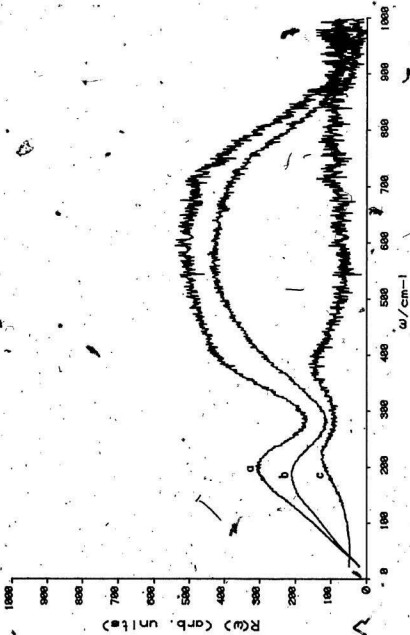
$\text{cm}^{-1}$  [12]. In the present study a single polarized band was observed at  $384 \text{ cm}^{-1}$  for saturated LiCl through the use of a difference spectrum (Fig. 13). The existence of a depolarized band at  $400 \text{ cm}^{-1}$  as claimed by Michaelson and Moskovits [38] was not observed. The authors report results from a difference spectrum between a pure water spectrum and the aqueous solution spectrum and it was assumed that the new bands arising were due solely to the interactions of the ions with water. This, of course, neglects the fact that the water spectrum itself may be different in the salt solution than it is in the pure state. Whether or not the band at  $384 \text{ cm}^{-1}$  is due to the  $A_1$  mode of the tetrahedral hydrate of the lithium ion or an ion aggregate symmetric stretch, of the type:



cannot be concluded without further isotope studies using the  $R(\omega)$  format for analysis. The shift of a polarized band at  $360 \text{ cm}^{-1}$  for  ${}^6\text{Li}^+$  to  $335 \text{ cm}^{-1}$  for  ${}^7\text{Li}^+$  in saturated chloride solutions reported by Nash [12] was assigned to solvent separated ion aggregates. The polarized bands were extracted from curve resolving of  $I(\omega)$  spectra. This technique can be unreliable in the low frequency region where background intensity from Rayleigh scattering is high. The original unresolved spectra reported by Nash are similar to those presented in this study.

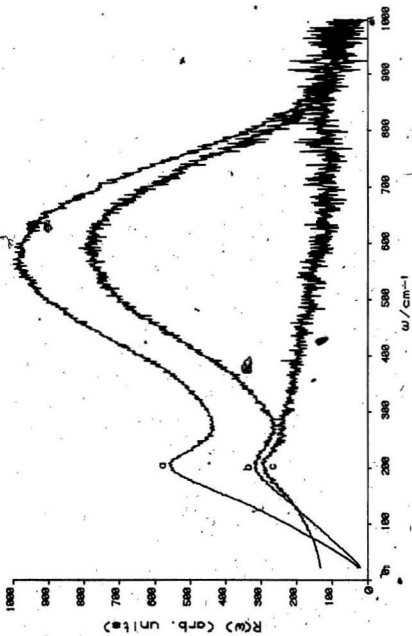
The  $R(\omega)$  spectra in Fig. 14 show the results for  $\text{CaCl}_2$ . A hexahydrate species has been assigned a  $\text{Ca}^{2+} \cdots 6\text{OH}_2$  stretch at about  $390 \text{ cm}^{-1}$  [39] but it is generally believed to be too weak to be seen. Unfor-

Fig. 13.  $R(\omega)$  spectra for saturated LiCl (aq).  $I_{VV}$  (a),  $I_{VH}$  (b) and  $I_{ISO}$  (c). The isotropic spectrum shows the hydrogen bond stretching mode at  $220\text{ cm}^{-1}$  and  $M\cdots O$  stretching at  $384\text{ cm}^{-1}$ .



5

Fig. 14.  $R(\omega)$  spectra for saturated  $\text{CaCl}_2$  (aq).  $I_W$  (a),  $I_{VH}$  (b) and  $I_{ISO}$  (c). The O...H-O stretching band appears at  $195 \text{ cm}^{-1}$  but no evidence of a discrete band arising from the stretching of the hydrated  $\text{Ca}^{2+}$  ion is observed.





tunately, no support is found from the  $R(\omega)$  spectrum for either viewpoint. Aside from the slightly polarized  $195 \text{ cm}^{-1}$  band, the difference spectrum shows only a broad slowly decreasing polarized signal continuing out to about  $700 \text{ cm}^{-1}$ .

#### Addition of anions

Anisotropic anions added to water can themselves give rise to low frequency Raman bands as well as affect the bands due to the water itself.  $\text{NO}_3^-$  has been shown to have a hindered rotational band at  $93 \text{ cm}^{-1}$  and  $\text{CN}^-$  a band at  $133 \text{ cm}^{-1}$  [7]. The depolarized spectra of saturated (8.10 m) aqueous  $\text{K}_2\text{CO}_3$  and 1 M aqueous  $\text{K}_2\text{CO}_3$  scaled as a function of concentration using the  $\text{CO}_3^{2-}$  band at  $1063 \text{ cm}^{-1}$  as an internal reference are shown in Fig. 15. Below  $350 \text{ cm}^{-1}$  two bands are observed and their frequencies are listed in Table 6.

Table 6  
 $I_{\text{VH}}$  data for  $\text{K}_2\text{CO}_3$   
 $\text{cm}^{-1}$

	$\nu_{\text{CO}_3^{2-}}$ hin. rot.	$\nu_{\text{O}\cdots\text{H}_2\text{O}}$ str	$\nu_1$
$\text{K}_2\text{CO}_3$ (sat.)	92 (22.3)	186 (236)	1063 (1000)
$\text{K}_2\text{CO}_3$ (1 M)	70 (6.4)	186 (61)	1063 (128)

Brackets contain relative intensities.

The shift in of the  $\text{O}\cdots\text{H}_2\text{O}$  stretch for water at  $186 \text{ cm}^{-1}$  to  $196 \text{ cm}^{-1}$  and the growth in intensity of this band with  $[\text{K}_2\text{CO}_3]$  are both results of increased hydrogen bonding in solution from a larger presence of  $\text{CO}_3^{2-}$ . With the spectra redrawn and intensities normalized to the  $\text{O}\cdots\text{H}_2\text{O}$  stretch band (Fig. 16), there is clear evidence for growth of the

Fig. 15.  $R(\omega)$  spectra of  $1 \text{ mol L}^{-1}$  and saturated aqueous  $\text{K}_2\text{CO}_3$  solutions from  $0 - 1000 \text{ cm}^{-1}$ . The saturated solution (8.10 m) (a) and the  $1 \text{ mol L}^{-1}$  solution (b) were intensity scaled as a function of concentration at the  $\text{CO}_3^{2-} \nu_1$  ( $1063 \text{ cm}^{-1}$ ). The increased intensity below  $300 \text{ cm}^{-1}$  for the saturated solution shows additional structuring of water to be dependent on the carbonate concentration.

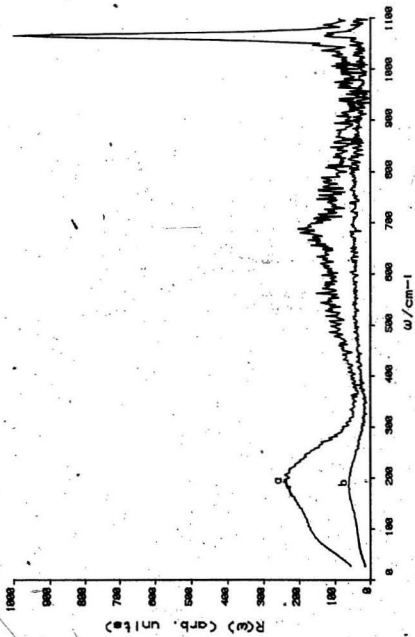
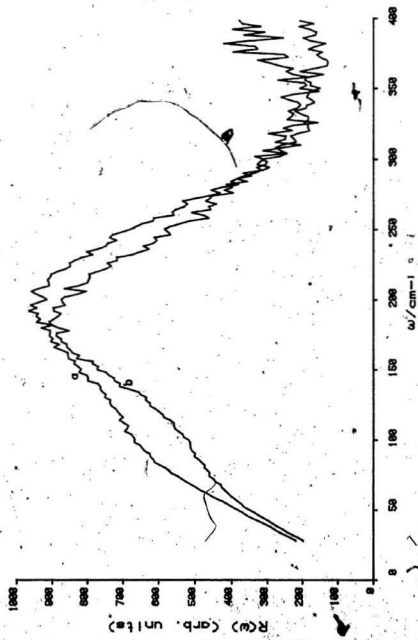


Fig. 16.  $R(\omega)$  spectra of  $1 \text{ mol L}^{-1}$  and saturated aqueous  $\text{K}_2\text{CO}_3$  solutions normalized to the O...H-O stretching mode of water. The spectra for saturated  $\text{K}_2\text{CO}_3$  (aq) (a) marks a growth in intensity at  $92 \text{ cm}^{-1}$  over that of the  $1 \text{ mol L}^{-1}$  solution (b) from the larger presence of hindered rotating  $\text{CO}_3^{2-}$  ions.



reorientational  $\text{CO}_3^{2-}$  band on the low frequency wing. In the 1M  $\text{K}_2\text{CO}_3$  solution the weak  $\text{CO}_3^{2-}$  band gives intensity at about  $70 \text{ cm}^{-1}$  compared to the  $\text{O}\cdots\text{H}-\text{O}$  bending mode of water at,  $68 \text{ cm}^{-1}$ . The band increased in intensity and gave a clear feature at  $92 \text{ cm}^{-1}$  in the saturated solution. This reported result for the librations of  $\text{CO}_3^{2-}$  is in close agreement with that reported for  $\text{NO}_3^-$ . The intensity of the reorientational peak due to  $\text{CO}_3^{2-}$  at  $92 \text{ cm}^{-1}$  is not as intense relative to the  $\text{O}\cdots\text{H}-\text{O}$  peak at  $196 \text{ cm}^{-1}$  as was observed for the  $\text{NO}_3^-$  peak at  $92 \text{ cm}^{-1}$ . This could be due to the small polarizability of  $\text{CO}_3^{2-}$  compared to  $\text{NO}_3^-$  or it could be due to an increase in the  $\text{O}\cdots\text{H}-\text{O}$  stretch intensity as a result of stronger hydrogen bonding with carbonate.

The presence of halides in solution does not give rise to any noticeable hindered anionic reorientational intensity as the anions are spherically symmetric and collision induced anisotropy is expected to be small. However, spherically symmetric anions can still affect the shape of the low frequency region of water as is shown in Figs. 17 and 18 and in Table 7.

Table 7  
Spectral data for aqueous halides

	$\nu_{\text{diff}} \text{ O}\cdots\text{H}_2\text{O str}$	$\nu_{\text{O}-\text{H}\cdots\text{X}^-}$	$\nu_{\text{O}\cdots\text{H}-\text{O str}}$	
			$\nu_{\text{W}}$	$\nu_{\text{H}}$
NaCl	187	-	183	178
KCl	181	-	176	171
KF	-	263	-	192

Aside from the higher intensity of the  $\text{O}\cdots\text{H}-\text{O}$  stretching band in KCl

Fig. 17.  $R(\omega)$  spectra for saturated aqueous NaCl.  $I_W$  (a),  $I_{VH}$  (b).  
The isotropic component (c) shows only the slightly polarized character of  
the  $O \cdots H-O$  stretch.

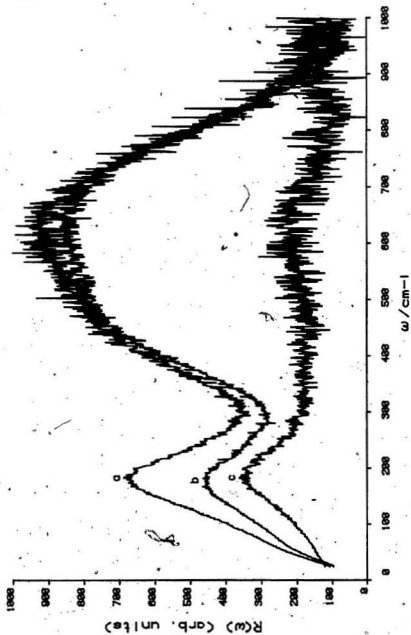
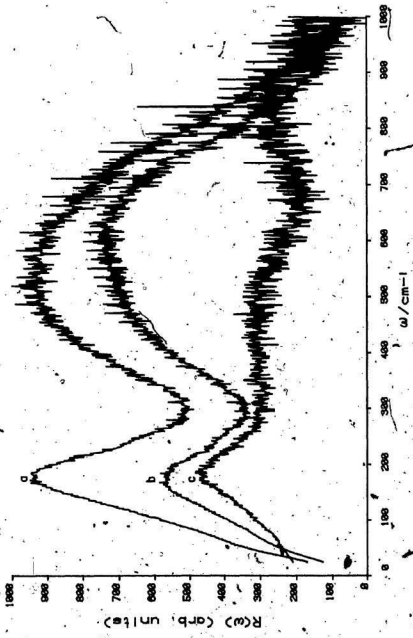




Fig. 18.  $R(\omega)$  spectra of saturated aqueous KCl.  $I_{VV}$  (a),  $I_{VH}$  (b).

As in the case of the previous figure only the O...H-O stretch is observed in the isotropic spectrum (c). The shift of the O...H-O stretch to  $176\text{ cm}^{-1}$  in the  $I_{VV}$  spectrum from  $183\text{ cm}^{-1}$  for NaCl (Fig. 17) is not enough evidence to suggest that this band arises from stretching of hydrated cations although there may be some secondary cation effects.

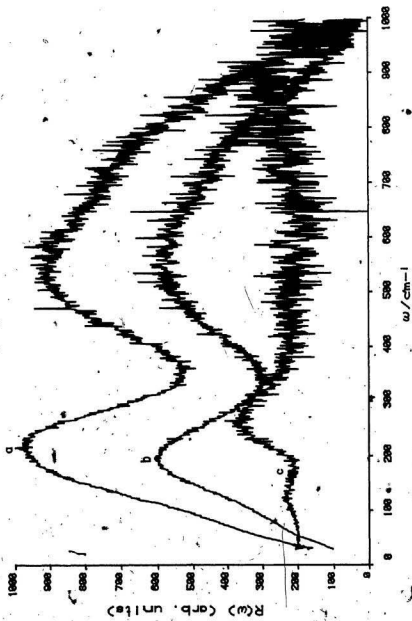
A



(such intensity differences are also noted in the I.R. [10]). No other differences are observed when compared to NaCl. The shift in frequency of this band is not enough evidence for cation-water interaction. Such interactions have been reported for these ions but at the same time Rayleigh scatter from chloride-water interaction was taken to be approximately zero [15]. This is contrary to Raman studies which suggest mostly anion-water contribution to the low frequency region. The present work suggests that the differences between the spectra for NaCl and KCl and the spectrum of water on page 18 are primarily due to anion-water interactions. Cation-water effects for  $\text{Na}^+$  and  $\text{K}^+$  may be present but they are very weak compared to those of  $\text{Li}^+$ ,  $\text{Mg}^{2+}$  and  $\text{Ca}^{2+}$  and are negligible compared to  $\text{Cl}^- \cdots \text{H}_2\text{O}$  interactions.

The spectrum of saturated aqueous KF is given in Fig. 19. Comparison of KCl and KF spectra shows changes in the contour of the  $\text{H}_2\text{O}$  librational region and a shift of the  $\text{O} \cdots \text{H}-\text{O}$  stretching band to  $218 \text{ cm}^{-1}$  for KF. Careful examination of the KF spectra reveals that the polarized and depolarized maxima in the  $200 - 300 \text{ cm}^{-1}$  region do not coincide suggesting the presence of a new polarized band for  $\text{KF}_{(\text{aq})}$ . The subtraction spectrum shows the presence of this new band at  $263 \text{ cm}^{-1}$ . The presence of this peak is further supported by the fact that the subtraction spectrum for  $\text{KCl}_{(\text{aq})}$  showed only the partly polarized  $\text{O} \cdots \text{H}-\text{O}$  peak at  $178 \text{ cm}^{-1}$ . The  $263 \text{ cm}^{-1}$  band of  $\text{KF}_{(\text{aq})}$  is not due to a collision induced restricted rotation of the  $\text{F}^-$  ion as such a band would also be present in the depolarized spectrum. Fluoride is spherically symmetric and is not expected to experience any torque from the surrounding media. The polarized band is assigned to a hydrogen bond stretching mode between  $\text{F}^-$  and  $\text{H}_2\text{O}$ . The  $192 \text{ cm}^{-1}$  band in the depolarized KF spec-

Fig. 19.  $R(\omega)$  spectra of saturated aqueous  $\text{KF}$ .  $I_{\text{VW}}$  (a),  $I_{\text{VH}}$  (b) and  $I_{\text{ISO}}$  (c). The difference in peak maxima of the  $\text{O}\cdots\text{H}-\text{O}$  water stretch in the  $I_{\text{VW}}$  and  $I_{\text{VH}}$  spectra indicates the presence of a new polarized band for  $\text{KF}$  (aq). The isotropic component confirms the existence of this peak at  $263\text{ cm}^{-1}$ . The peak is assigned to  $\text{O}-\text{H}\cdots\text{F}^-$  stretching.



1 R

trum is the anisotropic component of the partially polarized  $O \cdots H-O$  stretching mode.  $F^-$  is more strongly attracted to H than is the O of a water molecule and hence the tighter hydrogen bond with the fluoride ion gives rise to a higher stretch frequency. In terms of translation, this higher energy hydrogen bond means a more restricted movement of  $H_2O$ .

Hydroxide ion like the fluoride ion does not itself give rise to anisotropy in the low frequency region. Although not spherically symmetric, the size and polarizability and polarizability anisotropy of hydrogen is very small and additionally it is unlikely that the anion would experience any measurable torque from the surrounding molecules. The relevant data taken from the spectra of the aqueous alkali metal hydroxides is given in Table 8 and the  $I(\omega)$  spectra for these solutions appear in Figs. 20 - 26.

Table 8

$\nu_w$  data for aqueous hydroxides  
cm<sup>-1</sup>

	$\nu_{O \cdots H-O}$ str	$\nu_{O-H \cdots OH^-}$ str
LiOH (3.95M)	161	316
NaOH (10M)	172	298
KOH (11.5)	168	293
RbOH (5.86)	168	286
CsOH	?	277
NaOH (5M)	194	287
NaOH / NaClO <sub>4</sub> (5M in each)	194	-
NaOD	174	271

Fig. 20.  $I_{VV}$  (a) and  $I_{VH}$  (b) spectra for  $2.5 \text{ mol L}^{-1}$  LiOH (aq).

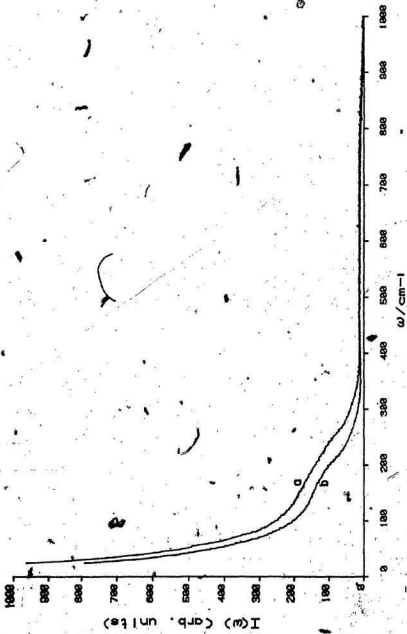




Fig. 21.  $I_W$  (a) and  $I_{VH}$  (b) spectra for  $3.95 \text{ mol L}^{-1}$  LiOH (aq).

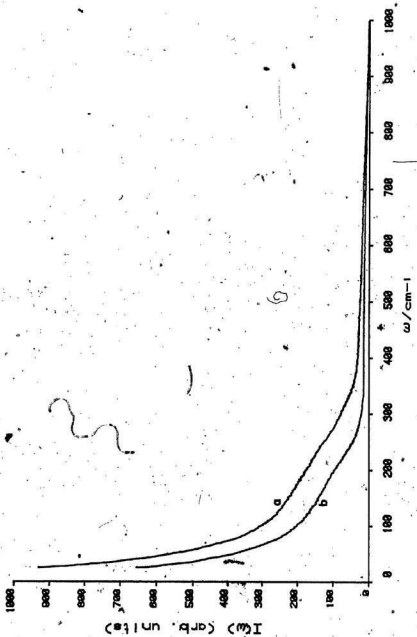


Fig. 22.  $I_W$  (a) and  $I_{VH}$  (b) spectra for  $10 \text{ mol L}^{-1}$  NaOH (aq).

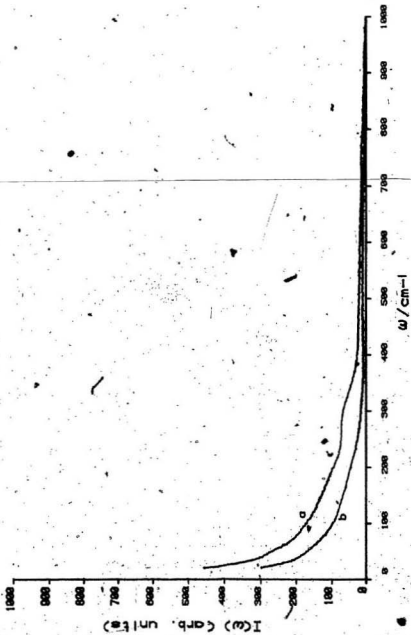


Fig. 23.  $I_{VV}$  (a) and  $I_{VH}$  (b) spectra for  $11.5 \text{ mol L}^{-1}$  KOH (aq).

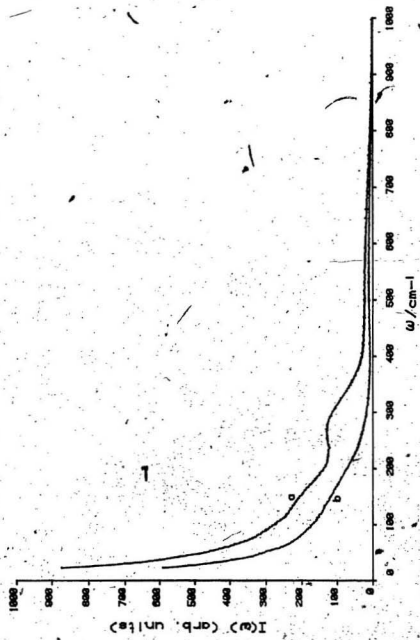
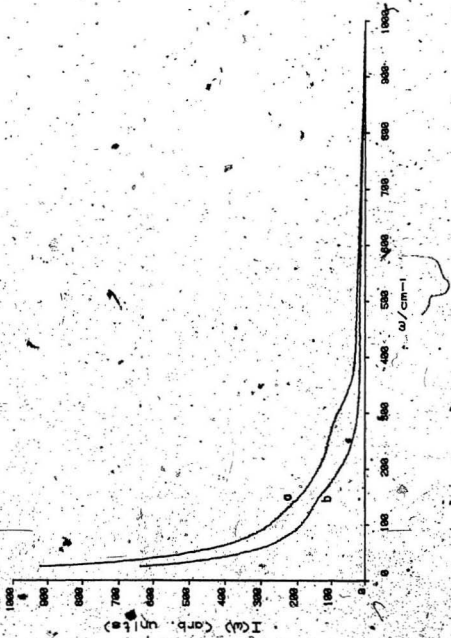


Fig. 24.  $I_{VV}$  (a) and  $I_{VH}$  (b) spectra for  $5.9 \text{ mol L}^{-1}$  ROH (aq).





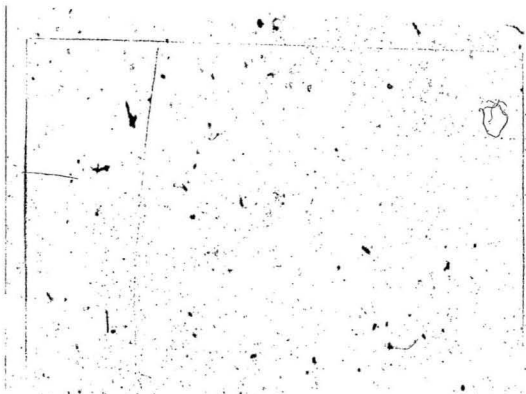


Fig. 25.  $I_W(\lambda)$  and  $I_{D1}(\lambda)$  spectra for  $8.6 \text{ mol L}^{-1} \text{ CaOH (aq)}$ .

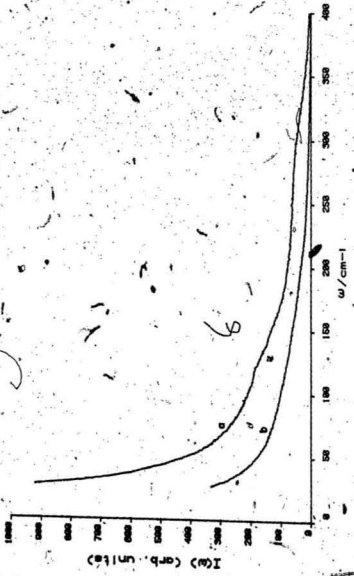
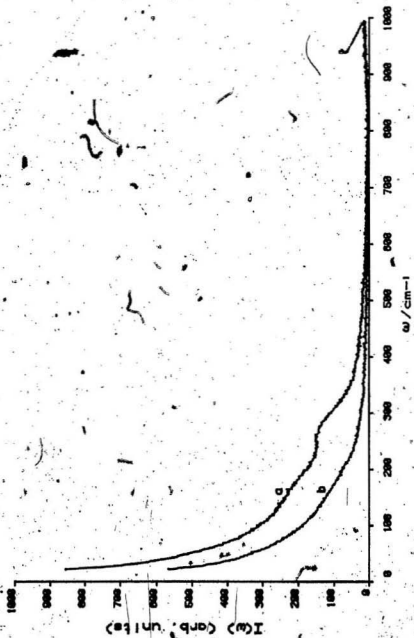


Fig. 28.  $I_{VV}$  (a) and  $I_{VH}$  (b) spectra for  $10 \text{ mol L}^{-1}$  NaOD (aq).



For the hydroxides of Na, K, Rb and Cs the spectra show polarized bands in the region of  $250 - 300 \text{ cm}^{-1}$ . Because the band in each case is polarized, it cannot be due to a libration of  $\text{OH}^-$ . These peaks are assigned to hydrogen bond stretches of the  $\text{H-O-H} \cdots \text{OH}^-$  complex and occur at  $298 \text{ cm}^{-1}$  for NaOH,  $293 \text{ cm}^{-1}$  for KOH and  $288 \text{ cm}^{-1}$  for RbOH (Figs. 28, 29, 30). The small differences in frequencies can be attributed to concentration effects and secondary effects of the cation on the water structure. Ion pairs of the type  $\text{M}^+\text{OH}^-$  would show a greater cation dependence than is observed and a tetrahedral species of the type  $\text{M}(\text{OH})_4^{3-}$  would be expected to have a force constant (and hence frequency) which was also very cation dependent. The relative intensities of the band would also be expected to be very cation dependent whereas the observed intensities are proportional only to the  $\text{OH}^-$  concentration. The  $\text{H-O-H} \cdots \text{OH}^-$  band for CaOH is present in Fig. 31, but the frequency reported ( $277 \text{ cm}^{-1}$ ) is low due to small  $[\text{OH}^-]$ . The amount of hydroxide present is not known for certain as a high degree of carbonate impurity was found (page 10). The low  $\text{OH}^-$  concentration compounded with a baseline subtraction at  $400 \text{ cm}^{-1}$  (not at a true zero) prevents an accurate frequency assignment.

In addition to  $\text{OH}^- \cdots \text{H}_2\text{O}$  interactions there is  $\text{H}_2\text{O} \cdots \text{H}_2\text{O}$  stretching present as indicated by the peaks at 172, 169, and  $168 \text{ cm}^{-1}$  for NaOH, KOH and RbOH respectively. The slight shift in this band may be due to secondary cation effects or to a weakening of the  $\text{H}_2\text{O} \cdots \text{H}_2\text{O}$  interaction due to the strength of the  $\text{OH}^- \cdots \text{H}_2\text{O}$  interaction. There may also be a small intensity contribution from the  $92 \text{ cm}^{-1}$  band of  $\text{CO}_3^{2-}$  impurity (see page 10). This is similar to the case of aqueous KF where two types of hydrogen bonding were observed. The  $\text{OH}^- \cdots \text{H}_2\text{O}$  stretches are of

Fig. 27.  $R(\omega)$  spectra for  $10 \text{ mol L}^{-1} \text{ NaOH (aq)}$ . Data from the  $I_W$  spectrum (a) show the presence of a polarized band at  $298 \text{ cm}^{-1}$  completely absent from the  $I_{VH}$  transformed data (b). The polarized band is assigned to the  $\text{H-O-H}\cdots\text{OH}^-$  symmetric stretching mode. The  $\text{O}\cdots\text{H-O}$  stretching mode of water shifts to a lower frequency of  $172 \text{ cm}^{-1}$  in the depolarized spectrum which may be a result of weakened water-water interactions or from secondary cation effects.

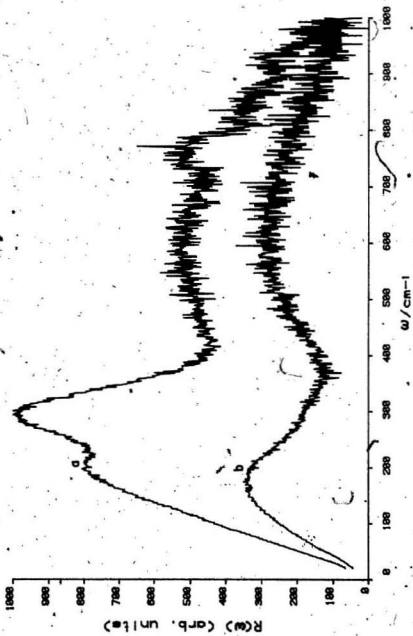


Fig. 28.  $R(\omega)$  spectra for  $11.5 \text{ mol L}^{-1}$  KOH (aq). The band at  $293 \text{ cm}^{-1}$  in the transformed  $I_{\text{VW}}$  spectrum (a) does not appear in the data obtained from the  $I_{\text{VH}}$  spectrum (b). This polarized band is assigned to symmetric stretching of the  $\text{H-O-H}\cdots\text{OH}^-$  unit. The  $\text{O}\cdots\text{H-O}$  stretching mode of water shifts to  $169 \text{ cm}^{-1}$  in the depolarized spectrum.



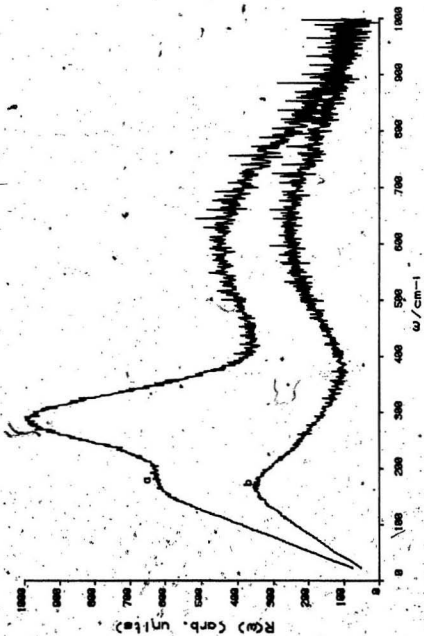


Fig. 29.  $R(\omega)$  spectra for  $5.9 \text{ mol L}^{-1} \text{ RbOH (aq)}$ . A polarized band at  $286 \text{ cm}^{-1}$  in the  $I_{\text{VV}}$  data (a) arises from the symmetric stretching of  $\text{H-O-H}^{\cdots}\text{OH}^-$ . The depolarized data appears in (b) showing only the  $\text{O}\cdots\text{H-O}$  stretch of water shifted to  $168 \text{ cm}^{-1}$ .

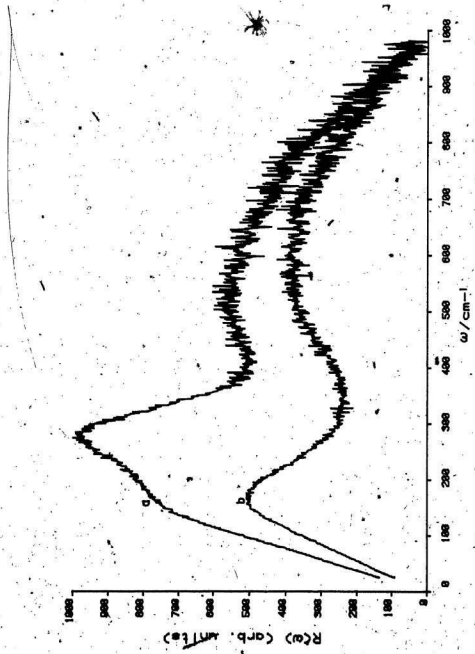


Fig. 30.  $R(\omega)$  spectra from ISO data for 10 mol L<sup>-1</sup> NaOH, 11.5 mol L<sup>-1</sup> KOH and 5.9 mol L<sup>-1</sup> RbOH, NaOH (a), KOH (b) and RbOH (c) show peaks at respectively 298 cm<sup>-1</sup>, 293 cm<sup>-1</sup> and 286 cm<sup>-1</sup>. Small frequency shifts are due to concentration and secondary cation effects.

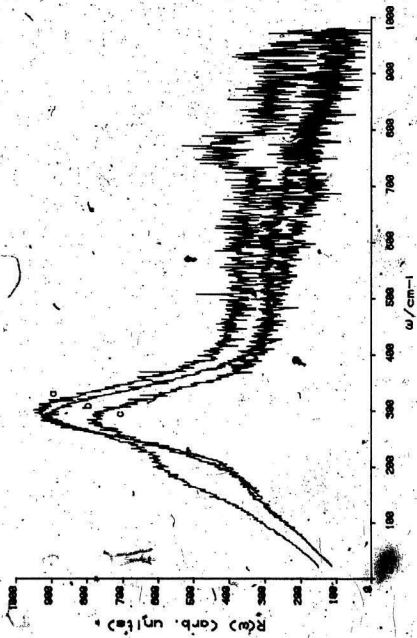
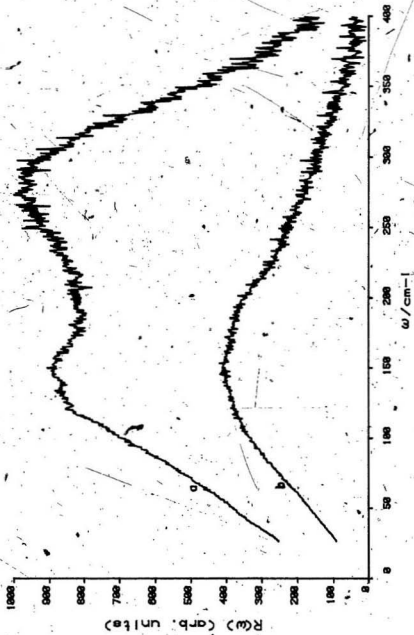
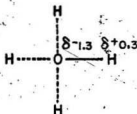


Fig. 31.  $R(\omega)$  spectra for  $8.6 \text{ mol L}^{-1} \text{ CaOH (aq)}$ ,  $I_{\text{W}}$  (a) and  $I_{\text{H}}$  (b). The  $\nu_{\text{max}}$  for  $\text{H-O-H}\cdots\text{OH}^-$  stretching cannot be given with any certainty as the sample proved to have a high carbonate concentration. This fact along with a premature baseline subtraction at  $400 \text{ cm}^{-1}$  distorts the spectra and shifts the band positions of the active modes. The observed position of the hydroxide-water intermolecular stretch at  $277 \text{ cm}^{-1}$  is questionable for  $8.6 \text{ mol L}^{-1} \text{ CaOH (aq)}$ .



higher energy than those of  $F^-$  with  $H_2O$ . This implies that the  $H_2O$  translation is even more restricted for hydroxide solutions than in fluoride solutions. In light of this, one might consider the following.  $F^-$  can H-bond to four hydrogens



whereas  $OH^-$  can only act upon three. Interference from other possible hydrogen bonds will be less for  $OH^-$ . Additionally, the overall negative charge on the F is lower than on the O of  $OH^-$  because the O-H bond of  $OH^-$  has additional bond polarity. The charge on  $F^-$  will be -1 but the charge on O in  $OH^-$  will be about -1.3. The net effect is that the oxygen will attract the hydrogens more strongly and hence a higher frequency for hydrogen bond stretching will result.

If the  $OH^- \cdots H_2O$  intermolecular separation is shorter than for  $F^- \cdots H_2O$ , a more negative partial molar volume would be expected for hydroxide solutions as the water would be less attracted to the fluoride. The partial molar volumes for  $OH^-$  and  $F^-$  in water are respectively -5.23 and  $-1.9 \text{ cm}^3 \text{ mol}^{-1}$  [40]. The negative molar volumes suggest strong hydrogen bonding for  $OH^-$  and  $F^-$ , while the more negative value for  $OH^-$  implies a very strong hydrogen bond.

The data for aqueous LiOH does not fit with the data for the other alkali metal hydroxides. The spectra in Figs. 32, 33 and 34 show polarized bands at  $247 \text{ cm}^{-1}$  and  $316 \text{ cm}^{-1}$ . The weak  $316 \text{ cm}^{-1}$  band has been assigned the  $H-O-H \cdots OH^-$  stretching mode. Most of the intensity



Fig. 32.  $R(\omega)$  spectra for  $2.5 \text{ mol L}^{-1}$  LiOH (aq).  $I_W$  (a) and  $I_{VH}$  (b).

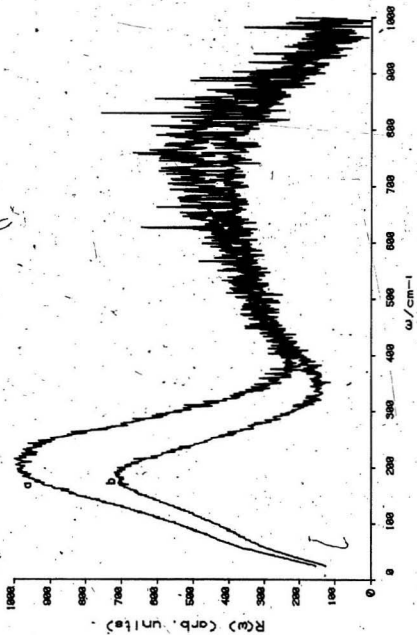


Fig. 33.  $R(\omega)$  spectra for  $5.95 \text{ mol L}^{-1}$  LiOH (aq).  $I_W$  (a) and  $I_{VH}$  (b).

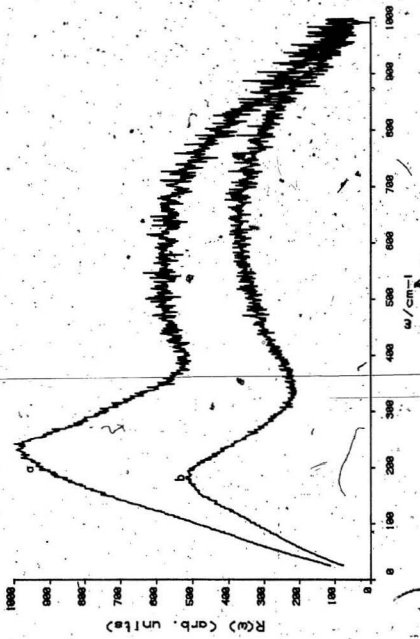
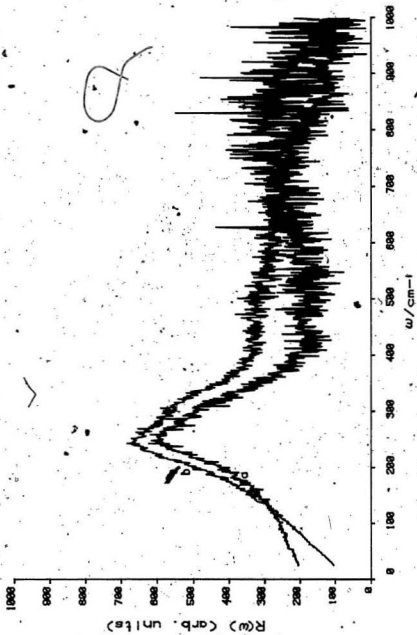


Fig. 34. Comparison of the  $R(\omega)$  isotropic components for (a) 2.5 mol  $L^{-1}$  and (b) 3.95 mol  $L^{-1}$  LiOH (aq). Growth of a weak polarized band at  $316\text{ cm}^{-1}$  is due to an increasing presence of  $H-O-H \cdots OH^{-}$  units. The polarized band at  $247\text{ cm}^{-1}$  is absent from the other alkali metal hydroxide solutions and possibly arises from  $Li^{+}OH^{-}$  ion pairs.



of the polarized bands is from the 247  $\text{cm}^{-1}$  peak and this band possibly represents the symmetric stretch of the  $\text{Li}^+\text{OH}^-$  ion pair. Moskovits and Michaelian [41] claim the presence of hydrated ion pairs in all the alkali metal hydroxide solutions but did not report the band at 247  $\text{cm}^{-1}$  for LiOH. Sharma [42,43] has also reported ion pairing for NaOH and KOH giving rise to polarized bands at 292  $\text{cm}^{-1}$  and 282  $\text{cm}^{-1}$  respectively but reports no evidence of ion pairing for LiOH. In the present work only LiOH shows ion pairing. This is consistent with the much lower solubility of LiOH in water compared to the other alkali metal salts.

The  $\text{OH}^- \cdots \text{H}_2\text{O}$  hydrogen bond stretch should exhibit normal isotope effects. The 298  $\text{cm}^{-1}$  band of NaOH shifts to 271  $\text{cm}^{-1}$  for NaOD in  $\text{D}_2\text{O}$  (Fig. 35). The bands of the librational region also shift to lower frequencies as with  $\text{D}_2\text{O}$ . The increase in intensity from 800  $\text{cm}^{-1}$  outward is from fluorescence of impurities and is apparent in Fig. 36.

The intensity of the  $\text{OH}^- \cdots \text{H}_2\text{O}$  hydrogen bond stretch increases with increasing  $[\text{OH}^-]$ . The spectra for 5M and 10M NaOH to 4000  $\text{cm}^{-1}$  is presented in Figs. 37 - 40. The symmetric stretch of the  $\text{OH}^-$  ion at 3606  $\text{cm}^{-1}$  increases in intensity from the 5M to the 10M solution. Increased intensity is also noted in the low frequency region indicating a larger presence of  $\text{OH}^- \cdots \text{H}_2\text{O}$  interactions. With the addition of  $\text{NaClO}_4$  to the 5M NaOH solution (Figs. 41 and 42), bands due to the tetrahedral  $\text{ClO}_4^-$  ion appear while the low frequency  $\text{OH}^- \cdots \text{H}_2\text{O}$  region seems to lose intensity and definition. In the O-H stretching region the intensity of the 3438  $\text{cm}^{-1}$  band drops and the 3233  $\text{cm}^{-1}$  band is more evident. This corresponds to a decrease in the number of hydrogen bonded water molecules and an increase in the number of "free" stretching water molecules. "Free" refers to the waters of hydration for  $\text{ClO}_4^-$  as

3

Fig. 35.  $R(\omega)$  spectra for  $10 \text{ mol L}^{-1}$  NaOD in  $\text{D}_2\text{O}$ .  $I_W$  (a) and  $I_{\text{OH}}$  (b). The hydroxide-water intermolecular stretch shifts to  $271 \text{ cm}^{-1}$  from that of  $298 \text{ cm}^{-1}$  for  $10 \text{ mol L}^{-1}$  NaOH (page 78). Impurities give rise to increasing intensity past  $900 \text{ cm}^{-1}$  as is evident in Fig. 36.



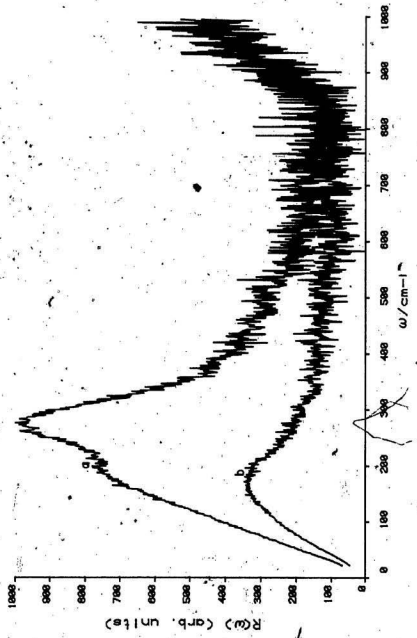


Fig. 36.  $R(\omega)$  spectra for  $10 \text{ mol L}^{-1}$  NaOD in  $\text{D}_2\text{O}$  showing increasing background intensity from fluorescing impurities.

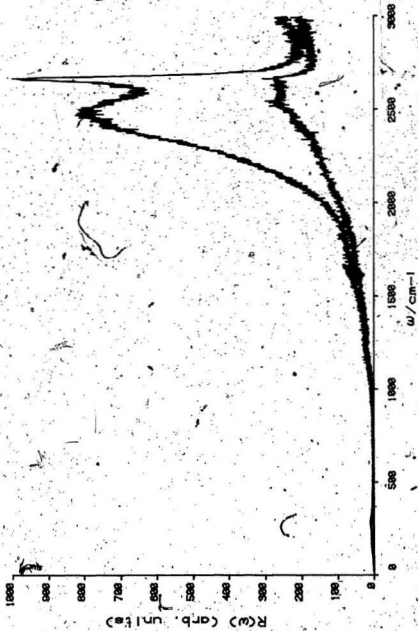


Fig. 37.  $I_{\text{W}}$  spectrum to  $4000 \text{ cm}^{-1}$  for  $5 \text{ mol L}^{-1}$  NaOH (aq).

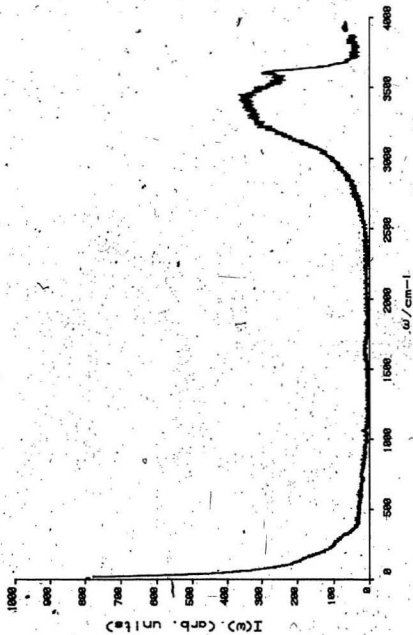


Fig. 38.  $^1W$  spectrum to  $4000\text{ cm}^{-1}$  for  $10\text{ mol L}^{-1}\text{ NaOH (aq)}$ .

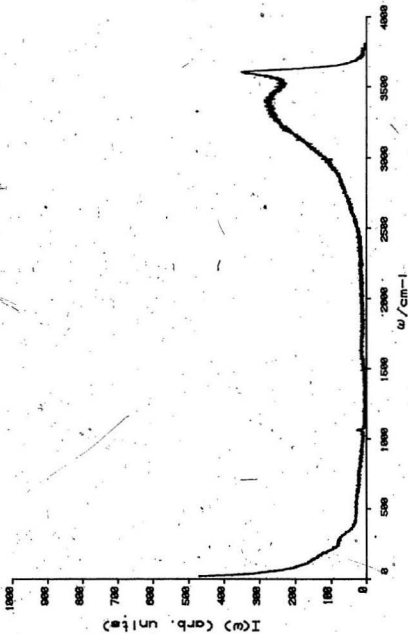


Fig. 39.  $R(\omega)$  spectrum to  $4000\text{ cm}^{-1}$  of  $I_W$  data for  $5\text{ mol L}^{-1}$  NaOH (aq).



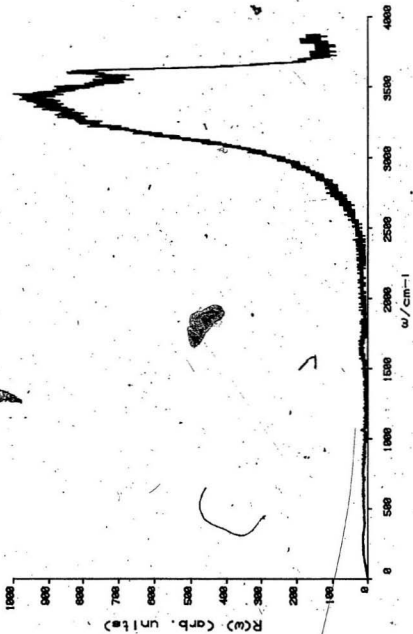


Fig. 40.  $R(\omega)$  spectrum to  $4000\text{ cm}^{-1}$  of  $I_W$  data for  $10\text{ mol L}^{-1}$  NaOH (aq). In comparison with Fig. 39 the growth of the  $\text{OH}^-$  intramolecular symmetric stretch is evident with increasing concentration. The carbonate impurity is seen to increase as the  $1063\text{ cm}^{-1}$   $\nu_1$  of  $\text{CO}_3^{2-}$  increases in intensity with the higher concentration of hydroxide.

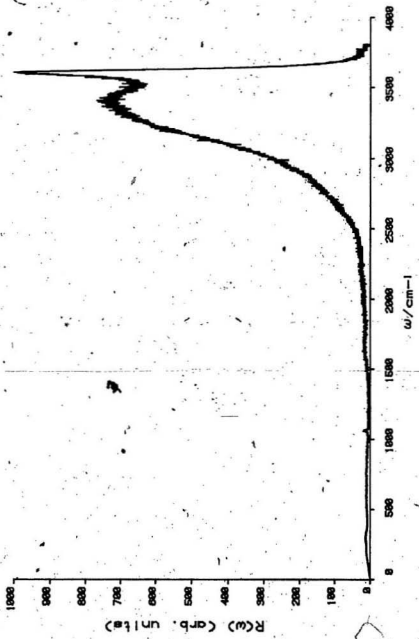
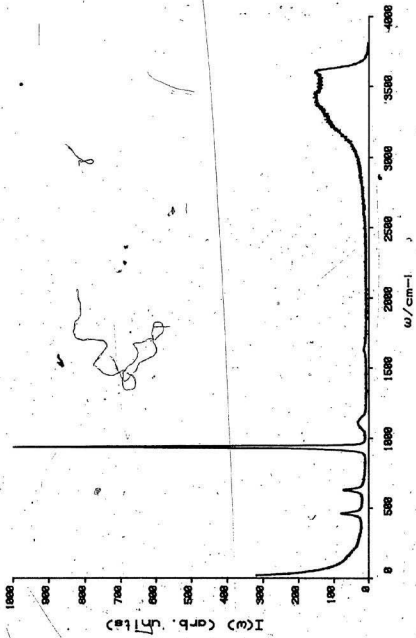
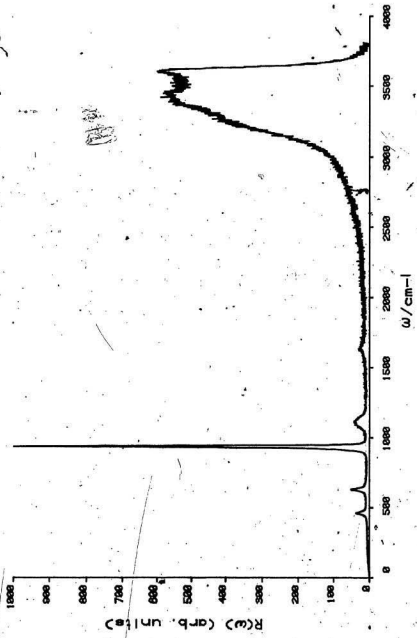


Fig. 41. -  $I_{\text{W}}$  spectrum of  $\text{NaClO}_4/\text{NaOH}$  (5 mol  $\text{L}^{-1}$  in each) to 4000  $\text{cm}^{-1}$ . In addition to the appearance of new bands from the internal modes of the perchlorate ion there, are changes in the spectrum of the  $\text{OH}^-$  solution itself in the area of intramolecular O-H stretching.



- 108 -

Fig. 42.  $R(\omega)$  spectrum of  $\text{NaClO}_4/\text{NaOH}$  (5 mol  $\text{L}^{-1}$  in each) to 4000  $\text{cm}^{-1}$  taken from  $I_{\text{W}}$  data. The internal modes of the perchlorate ion are visible between 300  $\text{cm}^{-1}$  and 1200  $\text{cm}^{-1}$ . The bands in the intramolecular stretching region change in relative intensity as the perchlorate ion breaks down the intermolecular structure. The intensity of the 3438  $\text{cm}^{-1}$  band drops relative to the 3233  $\text{cm}^{-1}$  band illustrating the loss of O-H stretching in water molecules hydrogen bonded to other water molecules or  $\text{OH}^-$  and an increase in the number of unassociated water molecules with O-H stretching. The loss of structure and intensity in the low frequency region also displays a loss of structure in the solution.



- 110 -

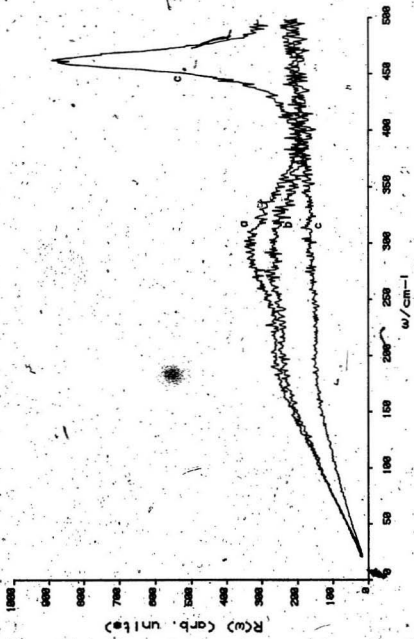
perchlorate-water interactions are weak. The spectra of the low frequency region for 10M NaOH, 5M NaOH and 5M NaOH/5M NaClO<sub>4</sub> normalized to the 3606 cm<sup>-1</sup> OH<sup>-</sup> band are shown in Fig. 43. The polarized OH<sup>-</sup>...H<sub>2</sub>O hydrogen bond stretch at 298 cm<sup>-1</sup> decreases in intensity with decreasing hydroxide concentration and is absent in the presence of perchlorate. The lower frequency O...H-O stretch for water-water interactions drops in intensity showing a loss of structure in the solution when ClO<sub>4</sub><sup>-</sup> is added. The absence of the 298 cm<sup>-1</sup> band in the hydroxide-perchlorate mixed solution spectrum confirms that this band is not cation dependent and cannot be due to ion pairs because the addition of NaClO<sub>4</sub> increases the cation concentration. Studies of a molten mixture of NaOH and KOH at 170°C also failed to show any evidence of a polarized peak in the 250 to 300 cm<sup>-1</sup> region a fact which further rules out ion pairs as the cause of the band in aqueous hydroxides [44].

#### CONCLUSION

In the present study use of the  $R(\omega)$  function has enabled relative intensities, peak frequencies and halfwidths to be determined with greater precision than has previously been possible for spectra presented in the  $I(\omega)$  format. This has greatly assisted the assignments and interpretations of spectral features. Studies of the hydrogen bond stretching mode of water showed shifts for substitutions of both H<sub>2</sub><sup>18</sup>O and D<sub>2</sub>O indicating an asymmetric OHO sequence. Hydrogen-bond stretching was also observed in aqueous metal fluoride and hydroxide solutions arising from an anion-water hydrogen bond stretching mode. These anion-water interactions proved to be much stronger than water-water interactions. A discrete metal-oxygen symmetric stretching band was observed in saturated solutions of LiCl and MgCl<sub>2</sub>. With the possible exception of aqueous LiOH, no ion



Fig. 43.  $R(\omega)$  spectra of  $5 \text{ mol L}^{-1}$  NaOH,  $10 \text{ mol L}^{-1}$  NaOH and  $\text{NaClO}_4/\text{NaOH}$  ( $5 \text{ mol L}^{-1}$  in each) taken from  $I_{\text{V}}$  data and normalized to the  $\text{OH}^-$  intramolecular stretch at  $3606 \text{ cm}^{-1}$ . The  $10 \text{ mol L}^{-1}$  NaOH spectrum (a) and the  $5 \text{ mol L}^{-1}$  NaOH spectrum (b) show an intensity dependence of the  $298 \text{ cm}^{-1}$  band on  $[\text{NaOH}]$ . When  $\text{NaClO}_4$  is present (c) this band disappears and the intensity of the  $\text{O}\cdots\text{H}-\text{O}$  stretch is lowered showing a drop in both water-hydroxide and water-water interaction. The assignment of the  $298 \text{ cm}^{-1}$  band to an  $\text{Na}^+\text{OH}^-$  ion pair would require an increase in the intensity of this band when  $\text{NaClO}_4$  is added due to the increased sodium ion concentration.



pairing was observed for any of the alkali metal salt solutions. A band originating from reorientational motions of the  $\text{CO}_3^{2-}$  anion was superimposed on the water spectrum in concentrated aqueous carbonate solutions.

The  $R(\omega)$  function has proven to be of considerable assistance in the identification of weak low frequency bands arising from scattering in liquids and glasses. The result of transforming the  $I(\omega)$  spectrum into the  $R(\omega)$  spectrum was a data set that is almost free of intensity from the exciting line an advantage which permits quantitative relative intensity studies for the low frequency region. Since the  $R(\omega)$  function is corrected for the effect of temperature on scattering intensity the  $R(\omega)$  data gives a spectrum which reflects only the  $\left(\frac{\partial \alpha}{\partial Q}\right)^2$  terms. This feature makes the  $R(\omega)$  function generally useful for studies of solids, liquids and molten salts. Although there is an apparent increase in noise with increasing  $\Delta\omega$  (this is a loss of S/N in the  $\omega=0$  band and not a deterioration of the S/N of the spectrum), the effect can be minimized with good signal averaging techniques. However, digitization of the noise may still be a problem if the recording device has a small dynamic range.

REFERENCES

- [1] G. E. Walrafen, *In Chap. 6 of "Water : A Comprehensive Treatise"*, (F. Franks, ed.), Vol. 1, Plenum Press, New York, N. Y. (1972)
- [2] D. E. Irish and M. H. Brooker, *In Chap. 8 of "Advances in Infrared and Raman Spectroscopy"*, (R. J. H. Clark and R. E. Hester, eds.), Vol. 2, Heyden, N. Y. (1976)
- [3] D. N. Waters, *In Chap. 2 of "Molecular Spectroscopy"*, Vol. 6, The Chemical Society, London (1979)
- [4] G. E. Walrafen, *J. Chem. Phys.* **36**(4), 1035 (1962)
- [5] J. Sandekar and B. Curnutte, *J. Mol. Spectrosc.* **58**, 189 (1975)
- [6] M. Moskovits and K. H. Michaelian, *J. Chem. Phys.* **69**(6), 2306 (1978)
- [7] M. H. Brooker and M. Perrot, *J. Chem Phys.* **74**(5), 2795 (1981)
- [8] D. I. Page, *In: Chap 9 of "Water : A Comprehensive Treaty"*, (F. Franks ed.), Vol. 1, Plenum Press, New York, N.Y. (1972)
- [9] N. Ohtomo and K. Arakawa, *Bull. Chem. Soc. Jap.* **51**(6), 1649 (1978)
- [10] O. F. Nielsen, *Chem. Phys. Lett.* **60**(3), 515 (1979)
- [11] M. A. Gray, T. M. Loehr and P. A. Pincus, *J. Chem. Phys.* **59**(3), 1121 (1973)
- [12] C. P. Nash, T. C. Donnelly and P. A. Rock, *J. Soln. Chem.* **6**(10), 663 (1977)
- [13] D. W. James and R. Irmer, *J. Raman Spectrosc.* **3**, 91 (1975)
- [14] D. W. James and R. L. Frost, *Farad. Trans 1*, **74**(3), 583 (1978)

- [15] C. Clement et G. Fourche, *J. Chim. Phys.* **77**(6), 545 (1980)
- [16] D. W. James and R. F. Armishaw, *Inorg. Nucl. Chem. Lett.* **12**, 425 (1976)
- [17] G. Brink and M. Falk, *Can. J. Chem.* **48**, 3019 (1970)
- [18] G. E. Walrafen, *J. Chem. Phys.* **52**, 4178 (1970)
- [19] M. Bennouna, H. Cachet, J. C. Lestrade and J. R. Birch, *Chem. Phys.* **62**, 439 (1981)
- [20] K. Abu-Dari, K. N. Raymond and D. P. Freyberg, *J. Am. Chem. Soc.* **101**:13 3688 (1979)
- [21] C. McM. Rohlfing, L. C. Allen, C. M. Cook and H. B. Schlegel, *J. Chem. Phys.* **78**(5), 2498 (1983)
- [22] C. J. Montrose, J. A. Bucaro, J. Marshall-Coakley and T. A. Litovitz, *J. Chem. Phys.* **60**(12), 5025 (1974)
- [23] R. H. Stolen, *Phys. Chem. Glasses* **11**, 83 (1970)
- [24] M. Hass, *J. Phys. Chem. Solids* **31**, 415 (1970)
- [25] R. Shuker and R. W. Gammon, *J. Chem. Phys.* **55**(10), 4784 (1971)
- [26] R. Shuker and R. W. Gammon, *Phys. Rev. Letters* **25**, 222 (1970)
- [27] D. D. Klug and E. Whalley, *J. Chem. Phys.* **71**(7), 2903 (1979)
- [28] P.-A. Lund, O. F. Nielsen, and E. Praestgaard, *Chem. Phys.* **28**, 167 (1978)
- [29] R. G. Gordon, *J. Chem. Phys.* **43**(4), 1307 (1965)
- [30] M. Perröt, M. H. Brooker, J. Lascombe, *J. Chem. Phys.* **74**(5), 2787 (1981)
- [31] J. W. Schultz and D. F. Hornig, *J. Chem. Phys.* **65**, 2131 (1961)

- [32] R. E. Weston. *Spectrochim. Acta* **18**, 1257 (1962)
- [33] G. E. Walrafen. In "Hydrogen Bonded Solvent Systems" (A. K. Covington and P. Jones, eds.). Taylor and Francis, London (1968)
- [34] H. D. Downing and D. Williams. *J. Geophys. Res.* **80(12)**, 1656 (1975)
- [35] R. M. Noyes. *J. Am. Chem. Soc.* **84**, 513 (1962)
- [36] J. T. Bulmer, D. E. Irish and L. Odberg. *Can. J. Chem* **53**, 3806 (1975)
- [37] S. P. Best, R. S. Armstrong and J. K. Beattie. *J. Chem. Soc. Dalton Trans.* 1655 (1982)
- [38] K. H. Michaellan and M. Moskovits. *Nature* **273**, 135 (1978)
- [39] M. H. Brooker and B. DeYoung, presented to the 58th Canadian Chemical Conference of the Chemical Institute of Canada, Toronto, May 1975
- [40] E. A. Moellwyn-Hughes. "Physical Chemistry". Pergamon, New York, N. Y. (1964)
- [41] M. Moskovits and K. H. Michaellan. *J. Am. Chem. Soc.* **102(7)**, 2209 (1980)
- [42] S. K. Sharma and S. C. Kashyap. *J. Inorg. Nucl. Chem.* **34**, 3623 (1972)
- [43] S. K. Sharma. *J. Chem. Phys.* **58(4)**, 1826 (1973)
- [44] M. H. Brooker and J. G. Shapter. *private communication*







